NASA Technical Memorandum 4217

Flow Visualization Studies
of Blowing From the Tip
# of a Swept Wing

Jeannette W. Smith, Raymond E. Mineck,
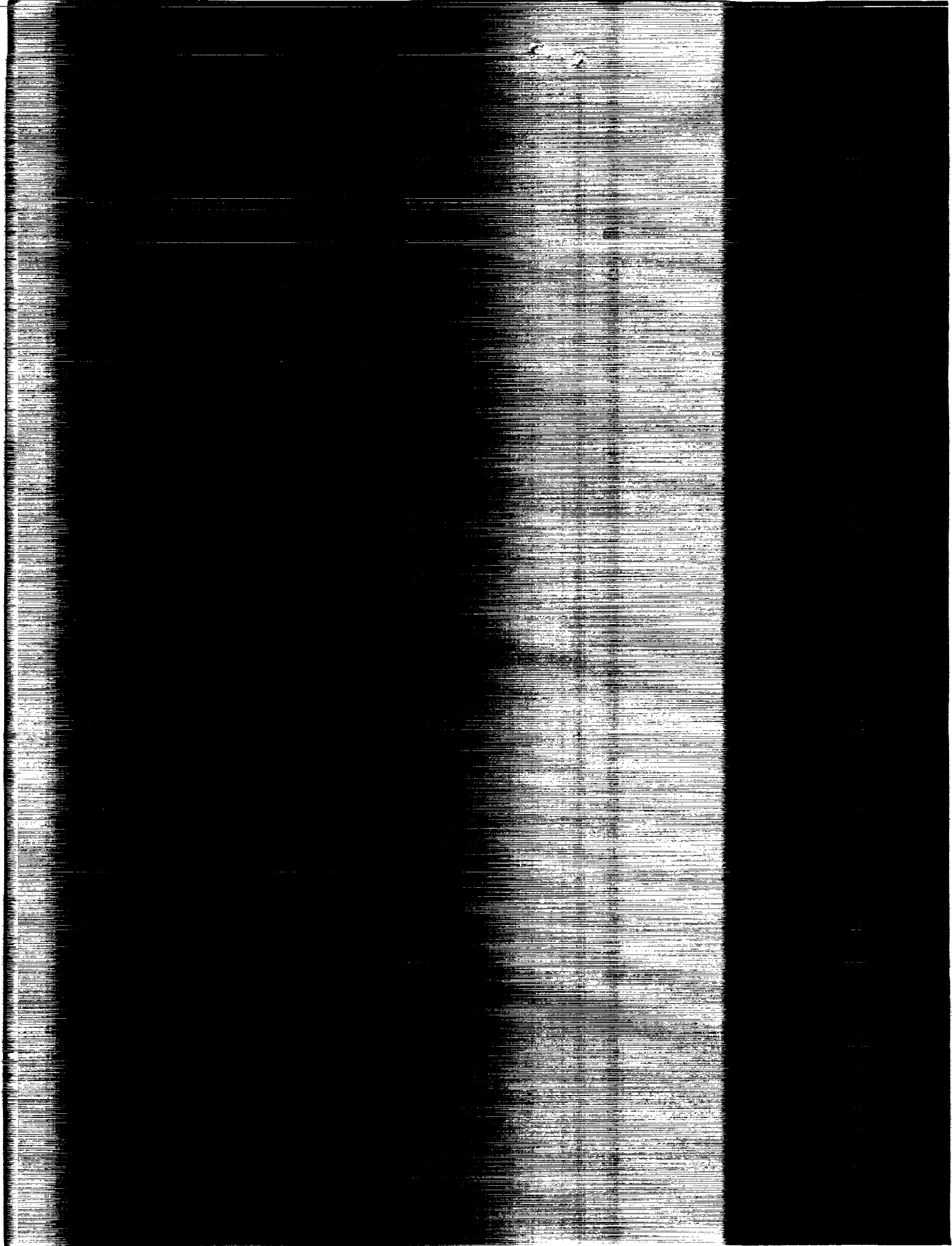and Dan H. Neuhart

NOVEMBER 1990

Flow Visualization Studies of Blowing From the Tip of a Swept Wing

Jeannette W. Smith and Raymond E. Mineck
Langley Research Center
Hampton, Virginia

Dan H. Neuhart
Lockheed Engineering & Sciences Company
Hampton, Virginia

Summary

Flow visualization studies of blowing from the tip of a swept wing were conducted in the Langley 16-by 24-Inch Water Tunnel. Four wing tips, each with two independent blowing slots, were tested. The two slots were located one behind the other in the chordwise direction. The wing tips were designed to systematically vary the jet length (jet chord), the jet in-plane exhaust direction (jet sweep), and the jet out-of-plane exhaust direction (jet anhedral). Each blowing slot was tested separately at two angles of attack and at four ratios of jet to free-stream velocity. Limited tests were conducted with blowing from both slots simultaneously. Blowing from the tip inhibited inboard spanwise flow on the upper wing surface near the tip. The jet path moved farther away from the tip as the ratio of jet velocity to free-stream velocity increased, and moved closer to the tip as angle of attack increased. Deflecting the jet downward or sweeping the jet aft reduced the jet spanwise penetration. At the same velocity ratio, the larger chord jet penetrated farther into the flow because of its larger momentum coefficient.

Introduction

Vorticity shed in the wake of a finite-length wing typically rolls up into a pair of counterrotating wing-tip vortices. The downwash induced on the wing by the wake is mostly the result of vorticity in the rolled-up wing-tip vortices. The downwash causes a rotation of the local lift vector, which will then have a component in the free-stream or drag direction. Different concepts have been tried to modify the form and rollup of the wake to reduce the induced drag. One concept, exhausting a jet at the wing tip in a spanwise direction, was originally developed to increase the lift on a low-aspect-ratio wing (refs. 1 and 2). Wake measurements behind a wing indicated that spanwise blowing from the tip reduced the intensity of the wing-tip vortex and displaced it outboard (ref. 3). The reduced intensity and the increased lateral separation of the wing-tip vortices should reduce the vortex-induced downwash on the wing and the induced drag. Early studies of this concept used blowing from jets with a length (or jet chord) that extended nearly the full length of the wing tip. The results in reference 3 indicate that locating the jet above the tip chordline or deflecting the jet downward (jet anhedral) was more effective in displacing the rolled-up tip vortex than locating an undeflected jet on the tip centerline. The jet momentum coefficients for these studies were large, with values up to 2.5. For the large mass flow rates associated with these high jet momentum coefficients, the ram drag

penalty is greater than the reduction in the induced drag. A technique which requires lower jet mass flow rates (and jet momentum coefficients) is desired.

Wu et al. (refs. 4 and 5) tested wing tips with several short-chord (or discrete) jets arranged in the chordwise direction instead of a single, continuous jet. Test results at lower momentum coefficients showed the same trends found with the single, continuous jet, although the magnitudes of the changes were smaller.

Previous studies indicated that blowing increases the local lift across the span of low-aspect-ratio wings (3 or less). The extent of the spanwise influence of the jet was not determined because of the small ratio of semispan to chord (1.5 or less). Further studies of the interaction of the tip-jet flow with the wing-tip vortex are needed on wings with larger aspect ratios. The purpose of the present study was to investigate wing-tip blowing on a moderate-aspect-ratio wing using relatively small jet momentum coefficients. In this report, results are presented from flow visualization tests on a moderate-aspect-ratio (5.7), swept wing with blowing at the tip. Different wing tips were used to vary the jet chord, chordwise position, sweep, and anhedral. The dye used to make different parts of the flow field visible failed to locate a well-defined, rolled-up, wing-tip vortex. The flow visualization results were restricted to the effect of spanwise blowing from the tip on the jet path and on the flow near the tip.

Symbols

A_j	jet exit area, ft^2
b	wing span, ft
b_j	extended span, ft, $b + \Delta b$
C_μ	jet momentum coefficient, $\dfrac{\dot{m}_j U_j}{0.5 \rho U_\infty^2 S}$
c_j	jet chord, in.
c_{tip}	tip chord, 2.2 in.
d_h	jet hydraulic diameter, $\dfrac{4A_j}{P}$, ft
$\dot{m}_j$	jet mass-flow rate, $\rho A_j U_j$, slugs/sec
P	jet exit perimeter, ft
R_d	jet Reynolds number based on hydraulic diameter
S	reference area of wing, ft^2
U_j	jet exit velocity, ft/sec
U_∞	free-stream velocity, ft/sec
WRP	wing reference plane
α	angle of attack measured from angle of zero lift, deg

Δb	extent of jet penetration, ft (see fig. 5(a))
δ_j	jet anhedral angle, deg
ρ	jet exhaust density, slugs/ft^3
ψ_j	jet sweep angle, deg

Test Description and Procedures

Test Facility

The Langley 16- by 24-Inch Water Tunnel was used for this test. A sketch of the tunnel is presented in figure 1(a). The tunnel has a vertical test section with a working length of about 4.50 ft. The velocity in the test section can be varied from 0 to 0.75 ft/sec, which results in unit Reynolds numbers from 0 to 7.73×10^4 per foot based on a water temperature of 78°F. The normal test-section velocity is 0.25 ft/sec. A sketch of the test section and the model support system is presented in figure 1(b). The model support system is mounted on a splitter plate and provides angular motion in two planes of rotation with ranges of $\pm15°$ and $\pm33°$. The center of rotation is on the centerline of the test section. Electric motors, mounted outside the tunnel, drive the model support system. The angle is set by using visual indicators with an accuracy of $\pm0.25°$. For these tests, the offset support and a wing splitter plate (fig. 1(b)) replaced the normal sting support. This offset support placed the wing tip 9 in. from the tunnel sidewall.

Model

The model consisted of a wing with four interchangeable wing-tip sections. Details of the wing are presented in figure 2. The planform was chosen to be representative of a business-jet wing or the outer portion of a commercial-transport wing. The span was selected to allow sufficient space for the flow from the tip jets to turn downstream without interference from the test-section sidewall. A constant HSNLF(1)-0213 airfoil section (ref. 6) was used. This 13-percent-thick, cambered airfoil section was designed for a lift coefficient of 0.2 at a Mach number of 0.7. For this test, the model attitude for zero lift was defined as 0° angle of attack. Rounded wing tips were formed by rotating the airfoil thickness about the airfoil camber line. The model was machined from aluminum and painted white to highlight the dyes used for flow visualization.

Four wing-tip sections with the same external shape, but with different jet slots, could be installed on the wing. Sketches of the four tip sections, identified as A, B, C, and D, are shown in figure 3. Photographs of the tip sections, with metal strips placed

in the jet exits to indicate the size and direction of the jets, are shown in figure 4. Each tip section had two plenum chambers. A sponge-like foam was placed in each plenum to reduce the turbulence in the jets and to help distribute the jet flow evenly. Two slots were cut into the tip to intersect each plenum, thereby forming the forward and aft jets. All the jet slots were 0.034 in. wide. On three of the tips, the slots were 0.14 in. long and were centered at the 30- and 60-percent-chord locations of the tip. On the remaining tip, the slots were 0.34 in. and 0.64 in. long and were centered at the 25- and 69-percent-chord locations of the tip. Tip A was considered the baseline, with a jet length of 0.14 in. and no sweep or anhedral. The lengths of the forward and aft slots were increased on tip B, the jets were deflected down 20° for tip C, and the jets were deflected down 20° and swept 30° aft for tip D. The jet parameters are summarized in table 1. Three dye orifices were installed in the forward portion of the tip section. They were located 0.09 in. above the top of the jet slots at 0.09, 0.41, and 0.78 in. downstream of the leading edge of the wing tip (fig. 3(b)).

Two tubes with a 0.19-in. inside diameter were installed in the wing to supply water to the forward and aft plenums. A flow-control valve and a flow-meter were placed in series with each supply tube outside the tunnel. A separate flowmeter measured the volume flow rate of water to each jet. A different color of dye was injected into each supply tube. The flow rate of the dye was fixed by the constant pressure in the dye reservoir with a needle valve. Blue dye was used for the forward jet, and green dye was used for the aft jet. Red dye was used for the three dye orifices located in the tip.

Procedures

The position of the rolled-up wing-tip vortex depends on the wing spanwise circulation distribution. Blowing from the wing tip modifies the local flow field, so that the spatial distribution of vorticity and the position of the rolled-up wing-tip vortex are changed. The wing lift and the jet momentum coefficients are directly related to the circulation and the blowing intensity, respectively. Therefore, the angle of attack, representing the wing lift, and the ratio of jet exit to free-stream velocity (or simply velocity ratio), representing the jet momentum, were selected as the primary variables of the test. Each tip was tested with the forward jet alone, the aft jet alone, and both jets operating simultaneously. A summary of the test conditions is presented in table 2. For each jet operating alone, two angles of attack and four velocity ratios were investigated. The two angles of attack were 0° and 5°. The higher angle of

attack produced the more visible wing-tip vortex with no wing-tip blowing. The four velocity ratios studied were 1, 2, 4, and 6. The higher values of 4 and 6 were included to duplicate the velocity ratios used in investigations of a jet in a cross wind (e.g., ref. 7). For the case with both jets operating simultaneously, the same two angles of attack and the same four velocity ratios were investigated. The velocity ratio was the same for the forward and aft jets. Also, at $\alpha = 0°$, four pairs of velocity ratios were tested for the forward and aft jets: 2 and 4, 2 and 3, 4 and 2, and 3 and 2.

In general, the tests were run at a free-stream velocity of 0.25 ft/sec. For tip B, tests of the aft jet operating at a velocity ratio of 1 were run at a free-stream velocity of 0.375 ft/sec because of limitations on the measurement accuracy of the flowmeter at low flow rates. When the test-section flow stabilized at the desired velocity, the model was set to the desired angle of attack. The valve for the tip-jet supply line was opened and adjusted to the desired flow rate. The desired flow rate was determined from the jet exit area, the density of the water, and the desired jet exit velocity.

The flow visualization data were recorded by using still color photography. After each change in angle of attack or velocity ratio, any transients were allowed to damp out before recording the photographs.

Results and Discussion

The effect of tip blowing on the flow field near the wing tip was investigated in this water-tunnel test. Attempts to visualize the rolled-up wing-tip vortex with the jets operating by using the dye orifices on the upper part of the wing tip were generally not successful. The weak wing-tip vortex was likely due to the low circulation generated by the small wing chord and small chord Reynolds number, which lead to separation on the aft part of the airfoil. However, the path of the jets was easily visible. Since previous studies indicated that blowing from the jet draws the wing-tip vortex outboard, the jet path should provide an indication of the movement of the wing-tip vortex. The jet path was quantified by a jet span that was defined as the span of the wing plus the spanwise extent of the jet as follows:

$$b_j = b + \Delta b$$

where Δb is the maximum spanwise extent of the visualized jet measured one tip chord downstream from the trailing edge of the tip. This change in span was measured from the photographs. These distances are identified in figure 5(a). The effect of

the velocity ratio, the angle of attack, and the slot size and orientation on the jet span were determined.

Studies of the path of a round jet exhausting into a uniform free stream generally use the ratio of the jet velocity at the exit to the free-stream velocity as the primary variable. This velocity ratio is used as the independent variable for most results presented herein.

Effect of Velocity Ratio

The effect of velocity ratio on the flow is presented in figures 5(a) to 5(d). These photographs show the plan view of tip B with both jets operating. Since the tip-jet water flow rate increases with the velocity ratio and the dye flow rate does not, the color of the jets becomes lighter with increasing velocity ratio. The jet flow and the wing-tip flow also become more turbulent and diffuse with increasing velocity ratio. The red dye injected from the orifices on the wing tip followed the flow close to the surface. The dye traces showed that the flow on the upper surface was drawn increasingly outboard and eventually into the jet as the velocity ratio was increased.

Distinct vortical structures such as the streamwise vortices shown in figure 6 for tip D and the periodic vortical loops shown in figure 7 for tip C were observed only at the lower velocity ratios of 1 and 2. The Reynolds number based on the hydraulic diameter for a velocity ratio of 2 is about 209 for each slot.

The thickness of the jet can be seen in the side-view photographs. (See fig. 8.) The thickness increases with increasing downstream distance. At a given downstream position, the jet thickness increases as the velocity ratio increases. The jet thickness can increase from 30 to 300 percent (depending on the tip) as the velocity ratio increases from 2 to 4.

As the velocity ratio increases, the jet momentum coefficient increases. Thus, at a given position downstream of the jet exit, the spanwise penetration of the jet increases as the velocity ratio increases. The increased spanwise penetration for one tip can be seen by comparing figures 5(a) to 5(d). There was increased penetration with increasing velocity ratio for all tip sections. The measured jet penetration or jet span one chord from the trailing edge of the tip is presented in figures 9(a) to 9(d). The increase in penetration with velocity ratio is not linear. The slopes of the jet penetration curves are greater when the velocity ratio is increased from 1 to 2 than when the velocity ratio is increased past 2.

Effect of Angle of Attack

At 0° angle of attack (no lift), the upper and lower surface pressures near the tip are nearly the same.

3

The flow near the surface is generally in the direction of the free stream, and no strong tip vortex is formed. The surface flow for the wing with no lift ($\alpha = 0°$) is shown in figure 10 for tip D. The dye paths from the forward part of the tip are generally aligned with the free stream as expected. With lift, the upper surface pressure is less than the lower surface pressure near the tip. The flow from the lower surface spills around the tip, and the flow near the upper surface moves inboard. The surface flow for the wing with lift ($\alpha = 5°$) is shown in figure 6 for tip D. With no wing lift, the jet exhausts into a relatively uniform flow field. With wing lift, the jet exhausts into the rotational flow field near the developing tip vortex. At a positive angle of attack, the jet path is above the wing plane (fig. 11), where the flow field is directed inboard because of the tip vortex. The jet span decreases as the angle of attack (lift) increases. This effect is seen by comparing the paths of the blue dye in figures 10 and 6. Also, the side view (fig. 11) shows how the flow from the forward jet rolls upward and inboard over the aft jet. The measured jet spans at the two angles of attack are presented in figure 12. The results generally follow the expected trend, except for a few instances at the higher velocity ratios.

Effect of Jet Slot Length

The effect of increasing the jet slot length for a given velocity ratio is presented in figure 12. As expected, the longer slot length (tip B) had the greater jet span. Although the jet velocity ratio is the typical variable used for investigations of a round jet, it does not account for differences in the jet area. Rectangular jets with different cross-sectional areas operating at the same velocity ratio have different jet momentum coefficients. A more appropriate way to compare jets with different slot sizes is to use the nondimensional jet force (jet momentum coefficient) C_μ as the primary variable. At the same velocity ratio, the longer jet slots have a greater momentum coefficient. This higher momentum implies greater spanwise penetration of the jet into the free stream. Thus, for a given value of C_μ, jets with different areas can be expected to produce the same force, and any differences in the spanwise penetration can be attributed to the jet shape. The variation of the nondimensional jet penetration $\frac{\Delta b}{b}$ with C_μ is presented in figures 13(a) and 13(b) for $\alpha = 0°$ and $\alpha = 5°$, respectively. The data are plotted on logarithmic scales, and most points lie within the band outlined by the dashed lines. The equations shown were determined from the slope and the intercept of each dashed line. The data for both jets blowing at

$\alpha = 0°$ and $\alpha = 5°$ showed similar trends and generally fell within the data band. The relationship shown between C_μ and $\frac{\Delta b}{b}$ indicates that for a given value of C_μ, roughly the same change in span is produced for either jet chord. However, for a given value of C_μ, larger jet velocities are required for the shorter slots.

Effect of Jet Direction

The effect of the jet direction on the jet span is presented in figure 14 for the wing-tip sections with the same jet chord. The effect of jet anhedral can be determined by comparing tips A and C. The differences in the span were generally small. With only the front jet on or only the rear jet on, deflecting the jet downward reduced the jet span. With both jets on, deflecting the jets downward generally did not affect the jet span. If the jet were exhausting into a uniform stream, deflecting the jet downward 20° should only rotate the jet path so that its penetration in the wing plane would be about 94 percent ($\cos 20°$) of the penetration of the undeflected jet. The results with the single jets are consistent with this simple analysis, but the results with both jets are not.

The effect of jet sweep can be determined by comparing tips C and D in figure 14. Generally, sweeping the jet aft (tip D) reduced jet span. The difference in the span was largest for both jets operating where the momentum was largest. Again, if the jet were exhausting into a uniform stream, the momentum normal to the tip in the wing plane would be reduced to $\cos 30°$ or 87 percent by sweeping the jet 30°.

Sweeping the jet aft changed the character of the jet. Photographs of the jet with and without sweep are presented in figure 15. The jet without sweep (tip C) was more diffuse and contained more widely spread vortical structures. At the lower velocity ratios shown, the jet with aft sweep (tip D) was well-defined and contained concentrated vortical structures. The vorticity associated with the swept jet is more closely aligned with the free stream than the vorticity associated with the unswept jet. This orientation causes the vortices to remain tighter in the case of the wing tip with the jet swept 30° aft.

Effect of Blowing Configuration

The jet spanwise penetration depends on the jet momentum and the flow field into which the jet exhausts. The forward jet and the aft jet exhaust into slightly different flow fields, especially when the lift is not zero. The momentum coefficient for both jets operating at the same velocity ratio is greater than the momentum for a single jet. Thus, the penetration for both jets should be greater than for

a single jet. The effect of the blowing configuration on the jet span is presented in figure 9. In general, the jet penetration for all tips was greatest for both jets operating. For the single jets with the same chord (tips A, C, and D), the penetration for the forward jet was slightly greater than for the aft jet. This is probably because the forward jet travels a greater distance to the measurement station and the spanwise penetration increases with the distance travelled. The aft jet penetrated farther for the longer chord jets (tip B) because the momentum coefficient is significantly larger for the aft jet.

The effect of using different jet velocity ratios for the forward and aft jets was also investigated at $\alpha = 0°$. Each tip was tested with the following combinations of forward and aft jet velocity ratio: 2 and 3, 2 and 4, 3 and 2, and 4 and 2. These differential jet results are shown in figure 9 by horizontal lines with a two-number label marking the level of extended jet span. The first number is the velocity ratio of the forward jet, and the second number is the velocity ratio of the aft jet. Except for the aft-swept jets (tip D), the combination of forward and aft velocity ratio of 2 and 4 had the largest penetration. The 2, 4 combination may have a generally larger penetration because the forward jet partially blocks the flow field, so that the velocity approaching the aft jet is reduced. The aft jet thus operates at an effective velocity ratio higher than if it were in the free stream and penetrates farther than an isolated jet would at the same velocity ratio.

Comparison of Measured and Empirical Jet Paths

Previous studies identified a pair of counterrotating vortices associated with the jet. These vortices were also visible at the lower velocity ratios in the present study. (See fig. 16.) Superimposed on these vortices are the laminar-vortex ring-type structures that are characteristic of laminar jets. The trajectory of the forward jet for tip A was calculated by using the empirical model of Thames and Weston (ref. 7). The calculated trajectory is shown in figure 17 superimposed over a plan-view photograph of the flow from the forward jet of tip A at a velocity ratio of 4 at an angle of attack of 0°. This calculated trajectory roughly follows the center of the visualized jet.

Conclusions

Flow visualization studies of spanwise blowing at the tip of a swept wing were conducted in the Langley 16- by 24-Inch Water Tunnel. The studies indicated the following results:

1. The jet flow draws the flow on the upper surface of the tip outboard. This flow moves farther outboard as the jet velocity ratio increases.
2. The spanwise penetration of the jet increases as the velocity ratio increases.
3. Deflecting the jets downward or sweeping the jets aft generally reduces the jet penetration.
4. For a particular jet momentum coefficient, the same increase in jet span is produced by larger or smaller slots. However, the smaller slots require larger jet velocities.
5. The spanwise penetration of the jet is generally reduced as the angle of attack is increased.
6. The wing-tip vortex could not be visualized because of effects associated with the small wing-tip chord.

References

1. Ayers, R. F.; and Wilde, M. R.: *An Experimental Investigation of the Aerodynamic Characteristics of a Low Aspect Ratio Swept Wing With Blowing in a Spanwise Direction From the Tips.* College of Aeronautics, Cranfield (England), 1956.
2. Smith, V. J.; and Simpson, G. J.: *A Preliminary Investigation of the Effect of a Thin High Velocity Tip Jet on a Low Aspect Ratio Wing.* Note ARL/A.163, Australia Dep. of Supply, June 1957.
3. Lee, C. S.; Tavella, D.; Wood, N. J.; and Roberts, L.: Flow Structure of Lateral Wing-Tip Blowing. AIAA-86-1810, June 1986.
4. Wu, J. M.; Vakili, A.; and Chen, Z. L.: Wing-Tip Jets Aerodynamic Performance. *ICAS Proceedings, 1982— 13th Congress of the International Council of the Aeronautical Sciences/AIAA Aircraft Systems and Technology Conference, Volume 2,* B. Laschka and R. Staufenbiel, eds., International Council of the Aeronautical Sciences, Aug. 1982, pp. 1115–1121. (Available as ICAS-82-5.6.3.)
5. Gilliam, Fred Thomas, Jr.: *An Investigation of the Effects of Discrete Wing Tip Jets on Wake Vortex Roll Up.* Ph.D. Thesis, Univ. of Tennessee, 1983.
6. Sewall, William G.; McGhee, Robert J.; Viken, Jeffery K.; Waggoner, Edgar G.; Walker, Betty S.; and Millard, Betty F.: *Wind Tunnel Results for a High-Speed, Natural Laminar-Flow Airfoil Designed for General Aviation Aircraft.* NASA TM-87602, 1985.
7. Thames, Frank C.; and Weston, Robert P.: Properties of Aspect-Ratio 4.0 Rectangular Jets in a Subsonic Crossflow. AIAA Paper 78-1508, Aug. 1978.
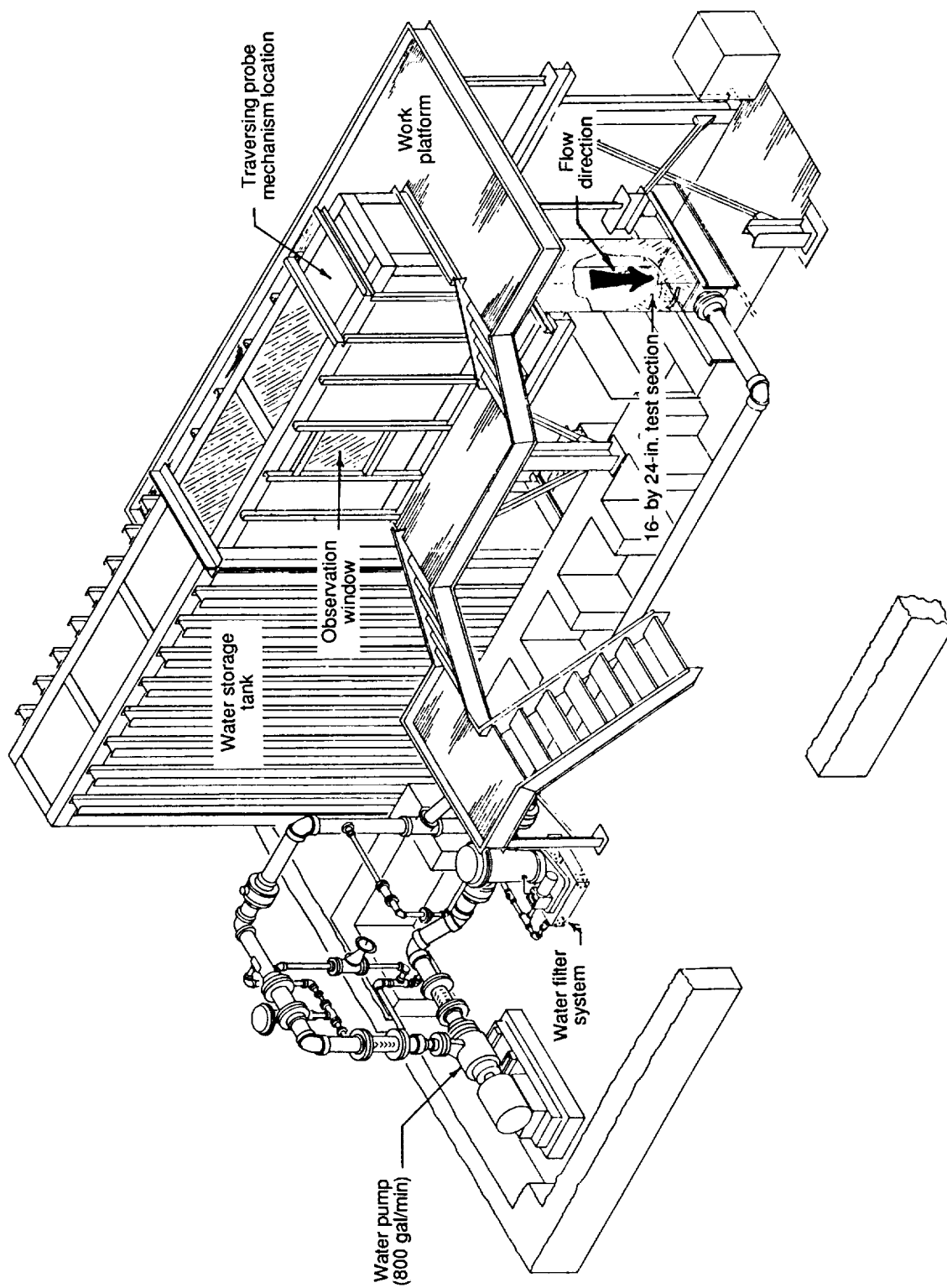
Table 1. Tip Characteristics

(a) Geometric parameters

Tip	Slot	c_j, in.	A_j, ft^2	P, ft	d_h, ft	δ_j, deg	ψ_j, deg
A	Either	0.14	3.31×10^{-5}	0.029	0.00456	0	0
B	Forward	.34	8.03×10^{-5}	.062	.00515	0	0
B	Aft	.64	1.51×10^{-4}	.112	.00538	0	0
C	Either	.14	3.31×10^{-5}	.029	.00456	20	0
D	Either	.14	3.31×10^{-5}	.029	.00456	20	30

(b) Flow parameters

U_j/U_∞	U_∞, ft/sec	Tip B (forward jet)		Tip B (aft jet)		Tips A, C, and D	
		C_μ	R_d	C_μ	R_d	C_μ	R_d
1	0.375	0.00028	177	0.00052	185	0.00011	157
1	.250	.00028	118	.00052	123	.00011	105
2	.250	.00111	236	.00208	247	.00046	209
4	.250	.00442	472	.00833	494	.00182	418
6	.250	.00995	709	.01873	740	.00410	628

Table 2. Angles of Attack Tested at Combinations of Forward and Aft Jet Velocity Ratios

U_j/U_∞ (aft jet)	Angle of attack, deg, at forward velocity ratio U_j/U_∞ (forward jet) of—					
	0	1	2	3	4	6
0	0, 5	0, 5	0, 5	-	0, 5	0, 5
1	0, 5	0, 5	-	-	-	-
2	0, 5	-	0, 5	0	0	-
3	-	-	0	0, 5	-	-
4	0, 5	-	0	-	0, 5	-
6	0, 5	-	-	-	-	0, 5

Traversing probe
mechanism location

Work
platform

Flow
direction

16- by 24-in. test section

Observation
window

Water storage
tank

Water filter
system

Water pump
(800 gal/min)

(a) Tunnel circuit.

Figure 1. Details of Langley 16- by 24-Inch Water Tunnel.

16 in.

24 in.

Flow

Splitter plate

Pitch mechanism (±15°)

Semispan wing

Offset support

Sting

Yaw mechanism (±33°)
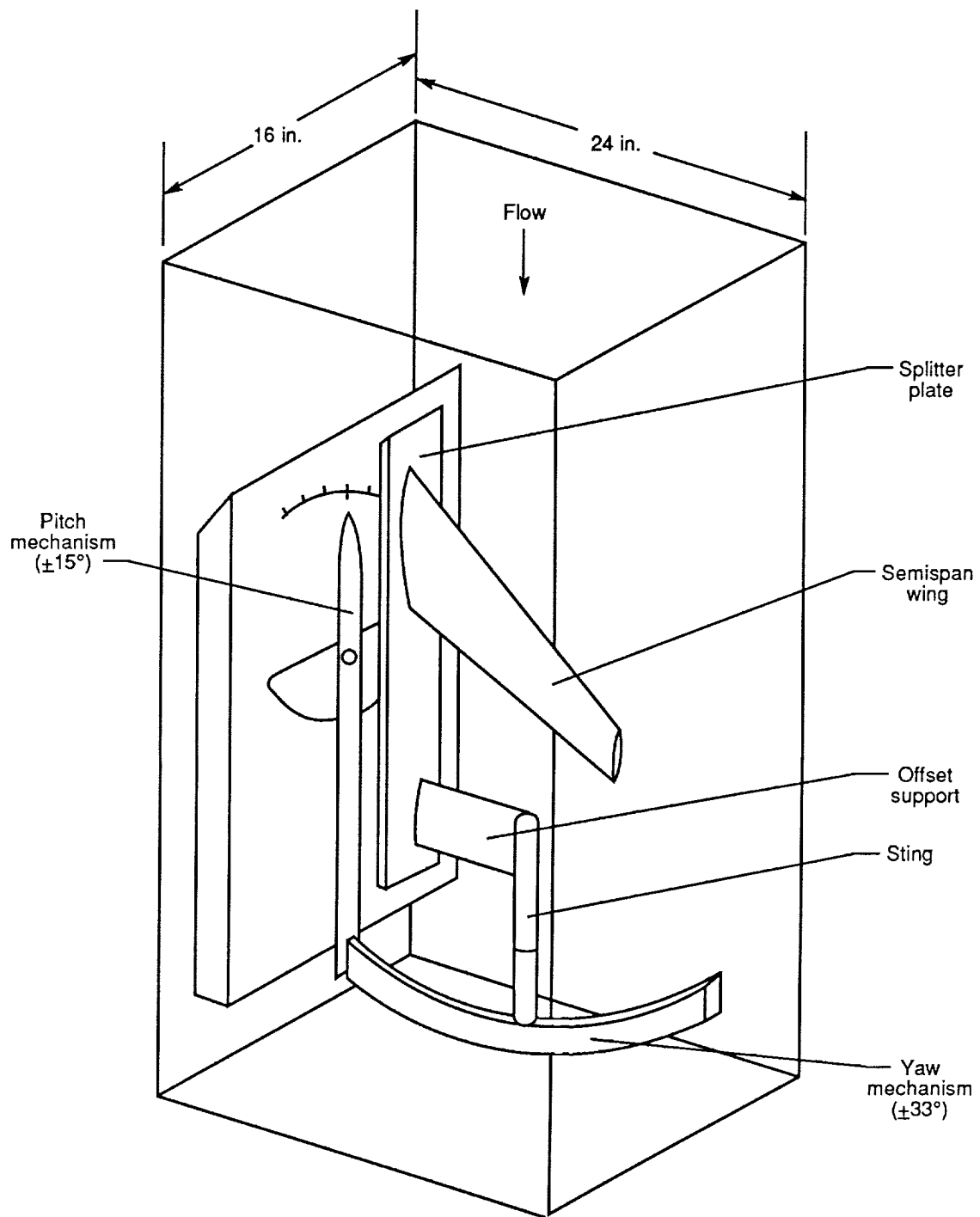
(b) Test section and model support system.

Figure 1. Concluded.

Figure 2. Details of wing.

Tip A
(baseline)

0.59

1.26

0.14

0.14

0.034

WRP

Tip B
(long-chord jet)

0.39

1.20

0.34

0.64

0.034

WRP

Tip C
(anhedral)

0.59

1.26

0.14

0.14

0.034

20° WRP

Tip D
(anhedral and sweep)

0.59

1.26

30°

0.14

30°

0.14

0.034

20° WRP

(a) Layouts of tips.

Wing upper
surface

0.09

0.09

0.41

0.78
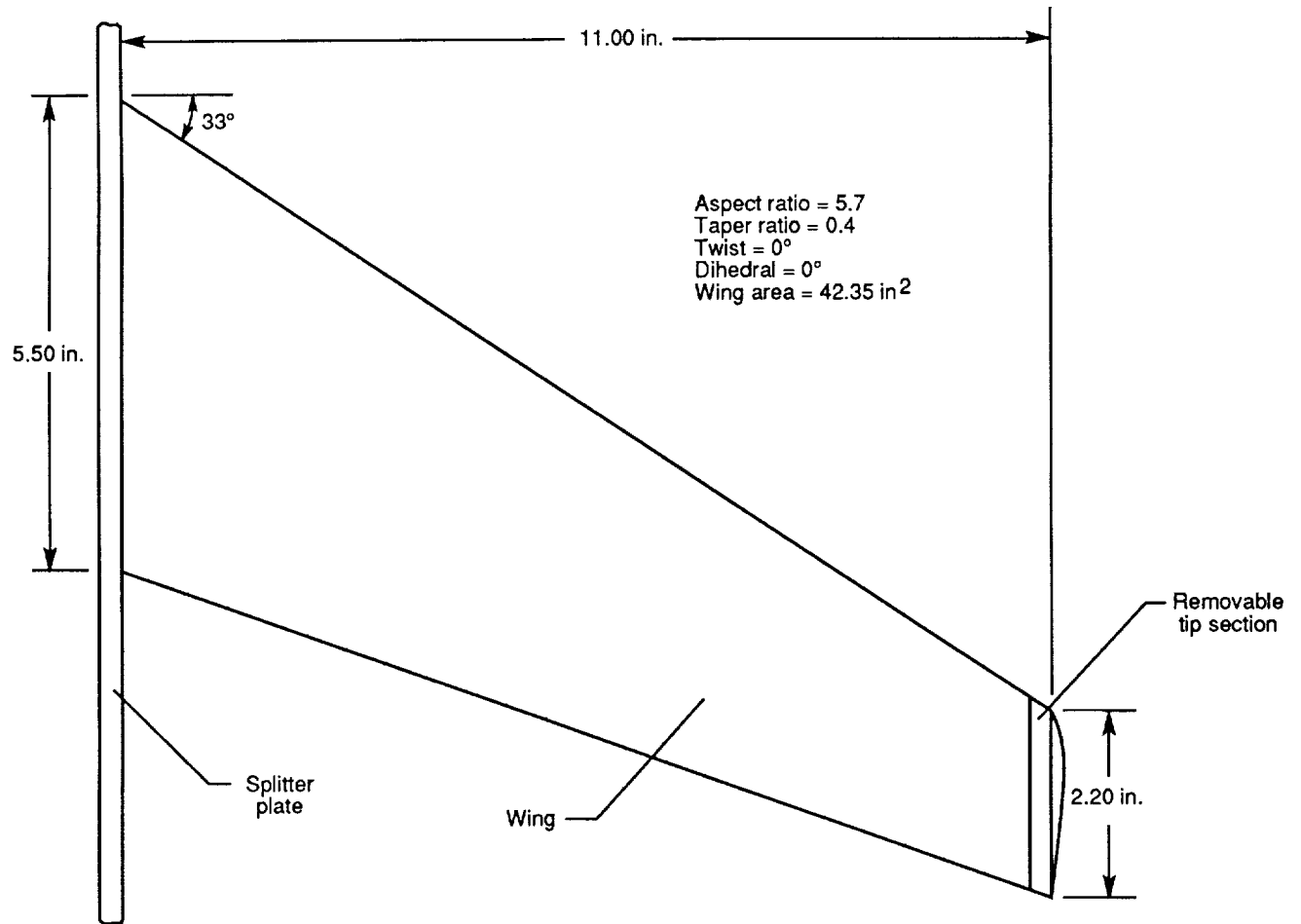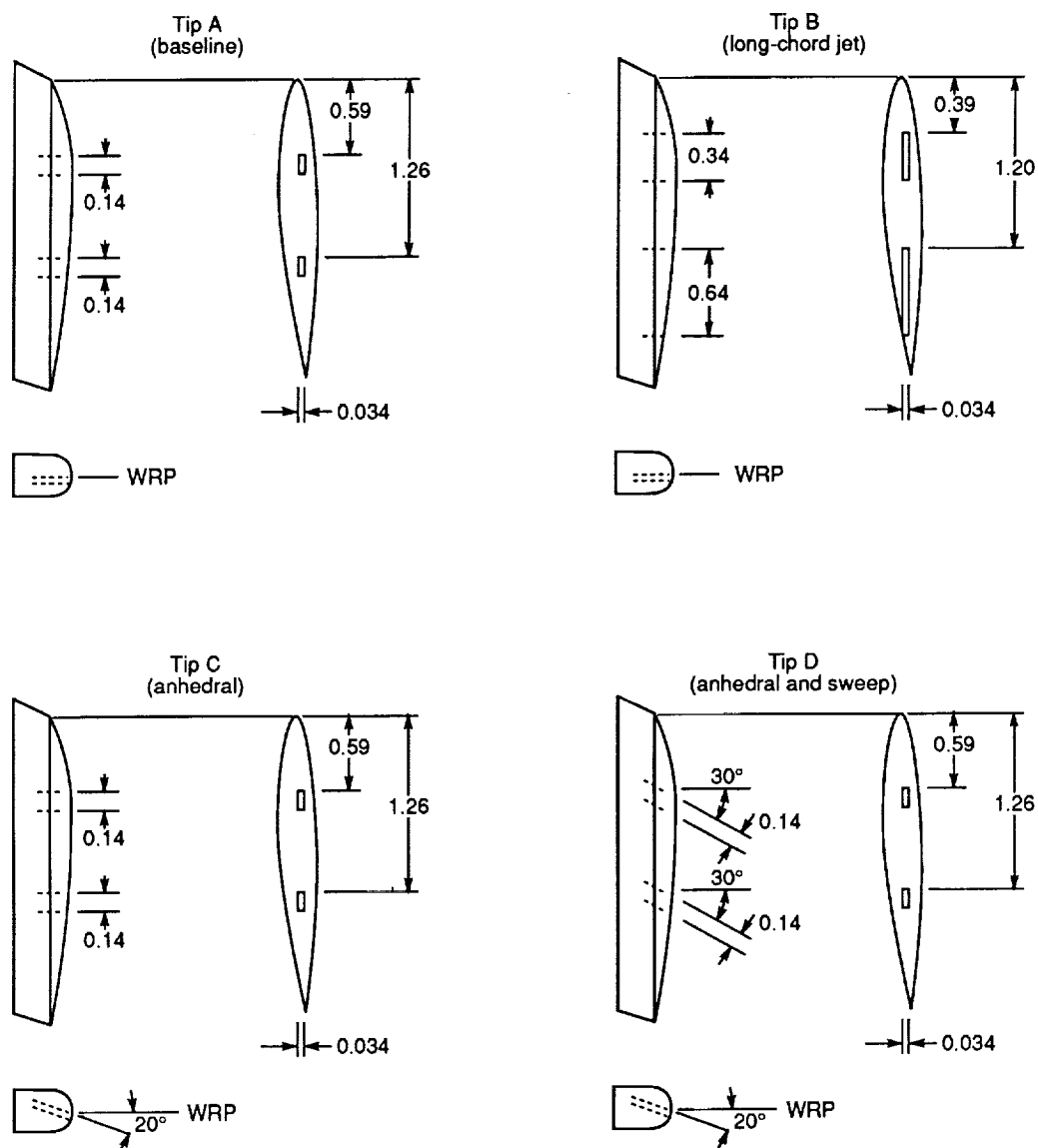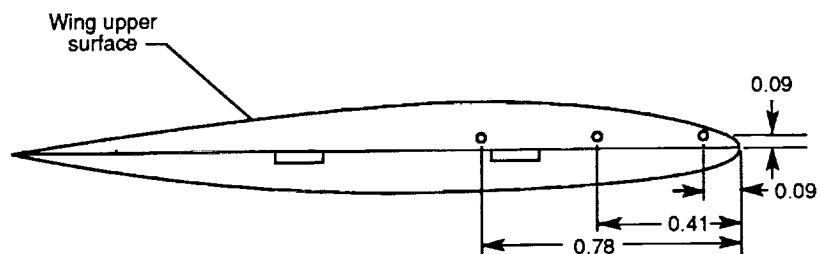
(b) Dye-port locations.

Figure 3. Details of removable tip sections. (All dimensions in inches unless otherwise specified.)

10
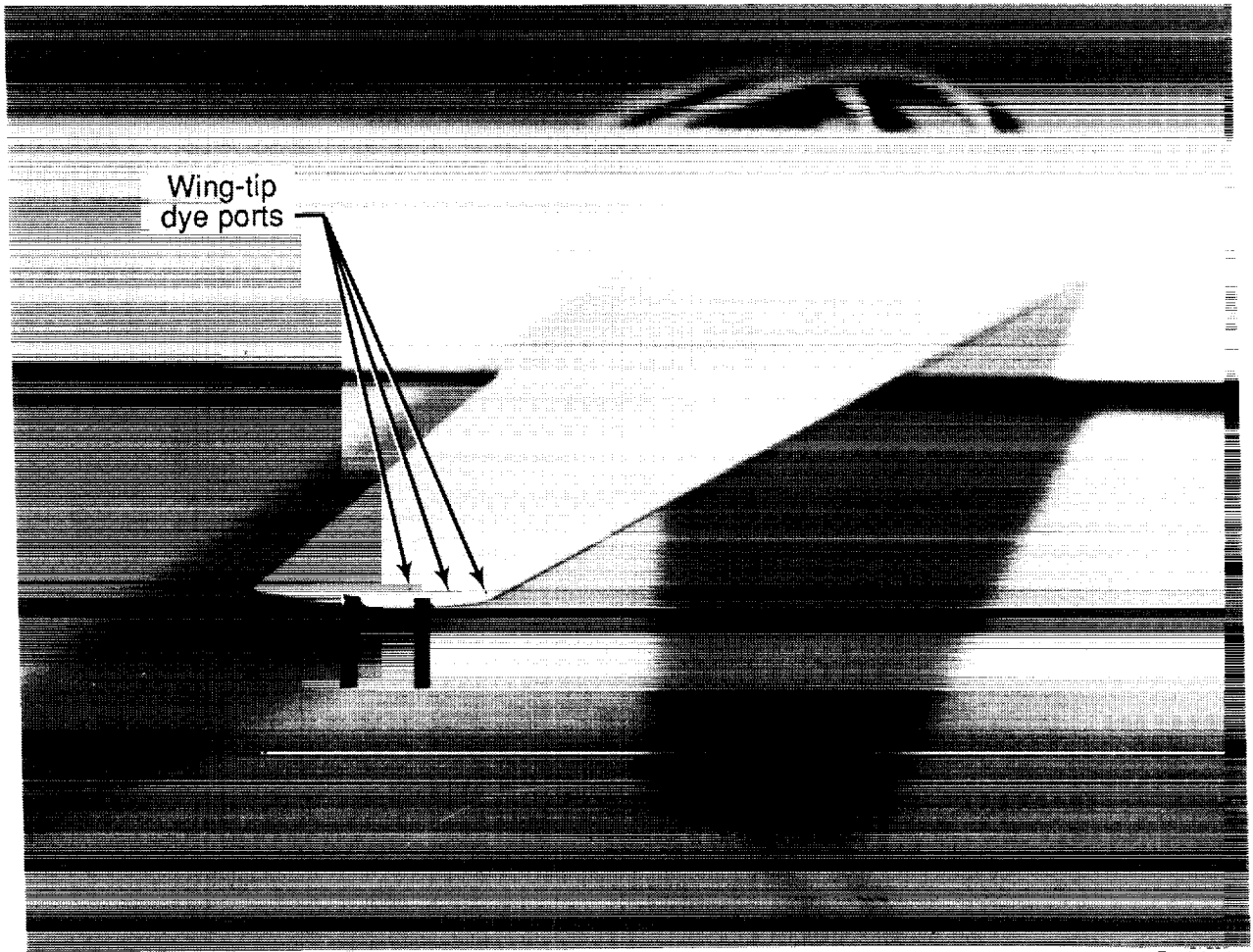
L-90-46

(a) Tip A.

Figure 4. Photographs of model and removable tip sections.

11
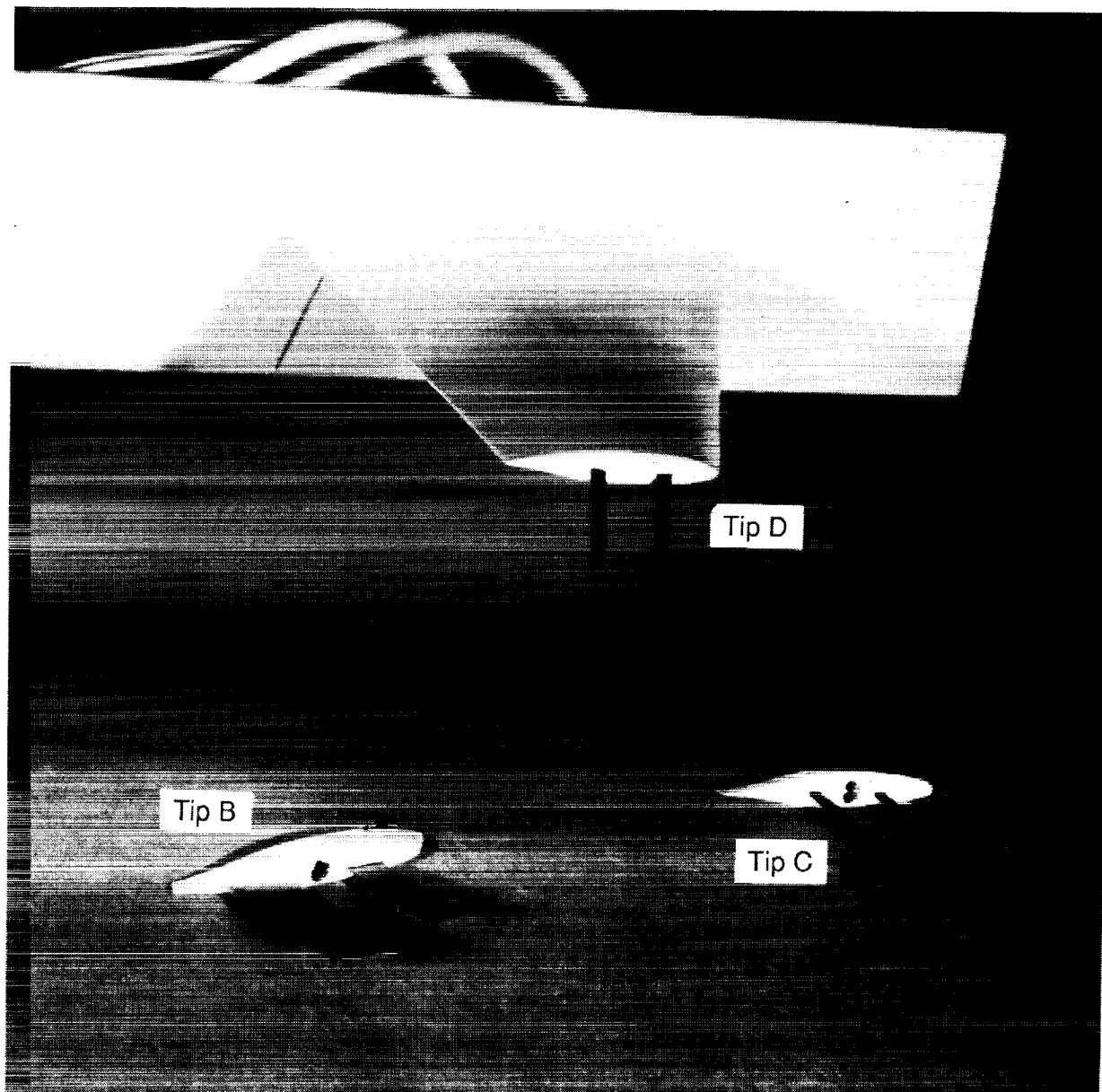
L-88-13,244

(b) Tips B, C, and D.

Figure 4. Concluded.

12

(a) $U_j/U_\infty = 1$ (forward and aft jets).

L-90-47

(b) $U_j/U_\infty = 2$ (forward and aft jets).

Figure 5. Effect of velocity ratio on flow near tip B with $\alpha = 0°$.

13
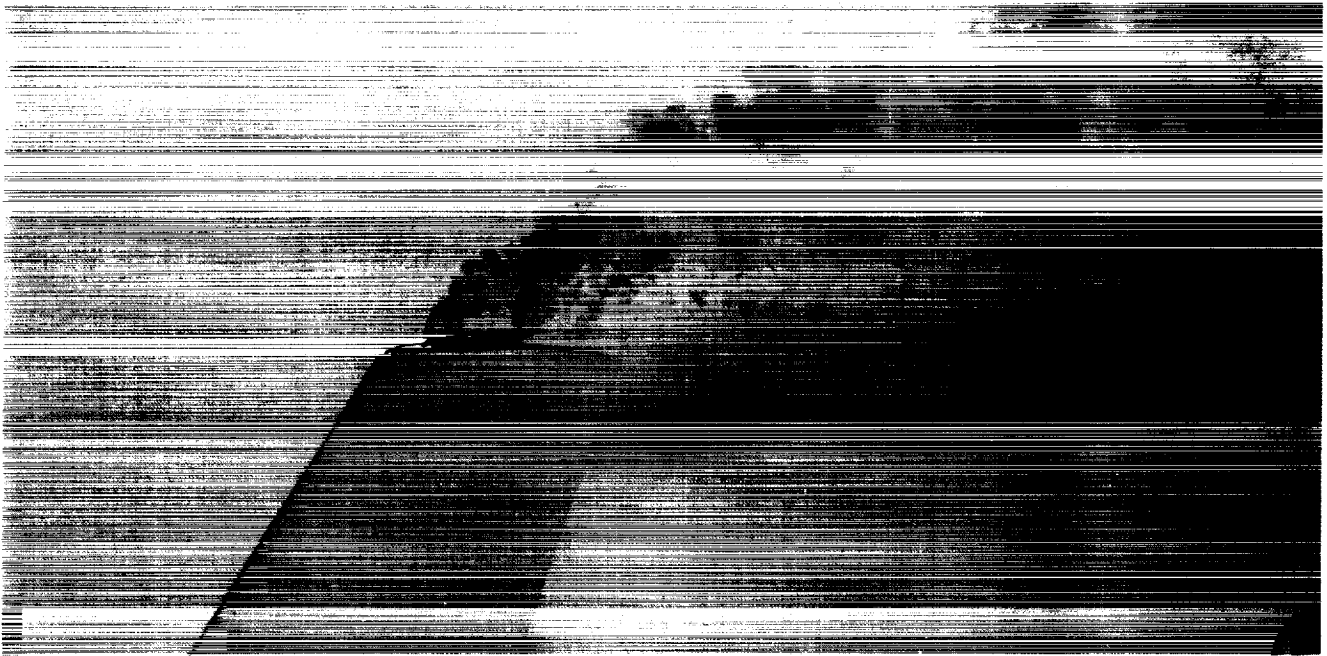
(c) $U_j/U_\infty = 4$ (forward and aft jets).
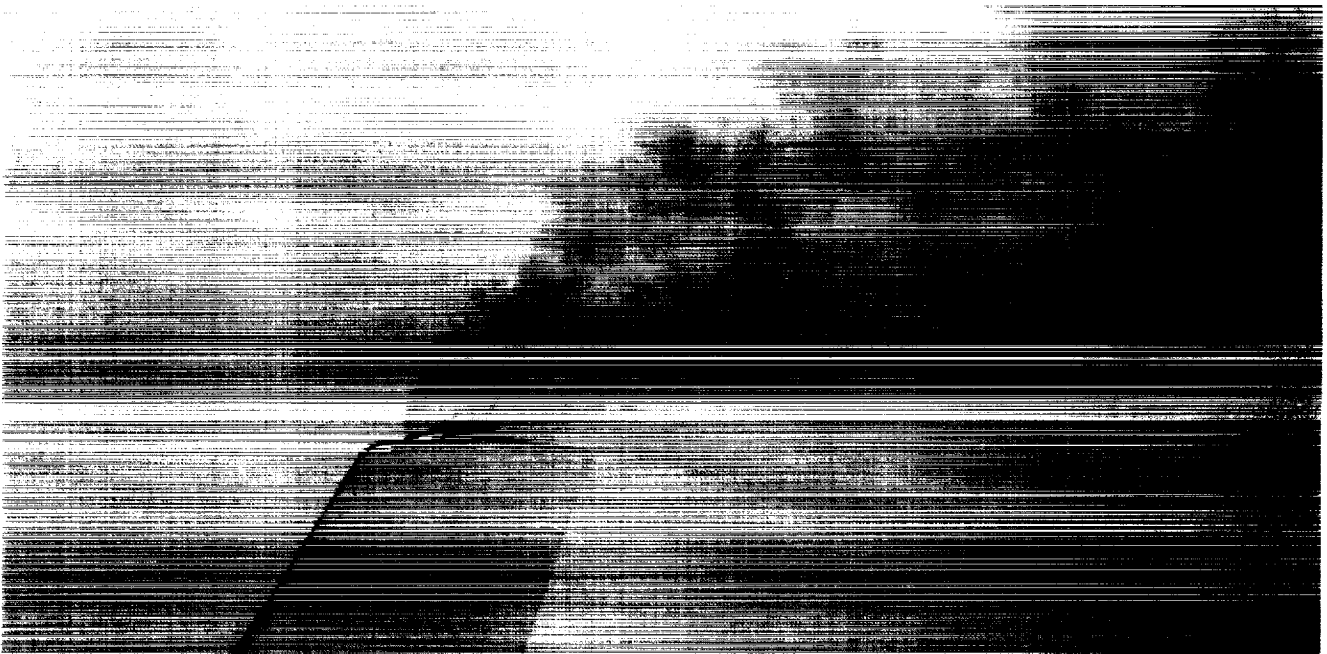
L-90-48

(d) $U_j/U_\infty = 6$ (forward and aft jets).

Figure 5. Concluded.

14
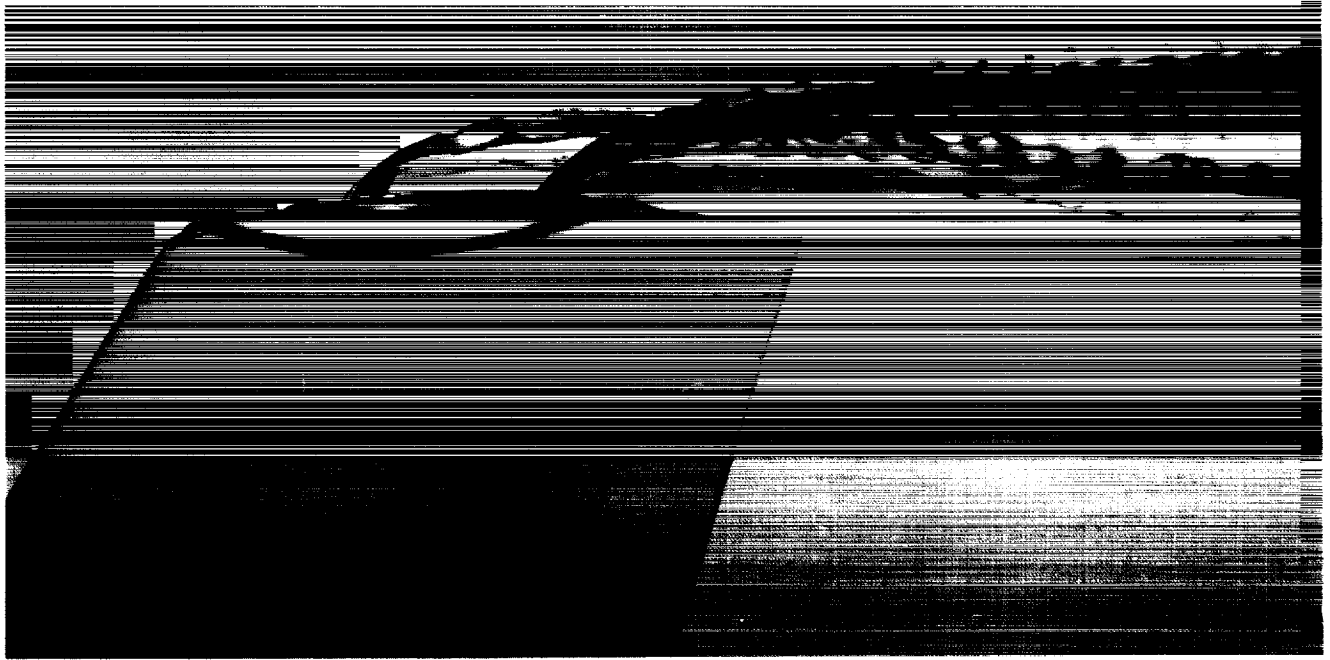
L-90-49

Figure 6. Plan view of flow near tip D with $\alpha = 5°$ and $U_j/U_\infty = 1$ (forward and aft jets).

L-90-50

Figure 7. Plan view of flow near tip C with $\alpha = 5°$ and $U_j/U_\infty = 1$ (forward and aft jets).

15
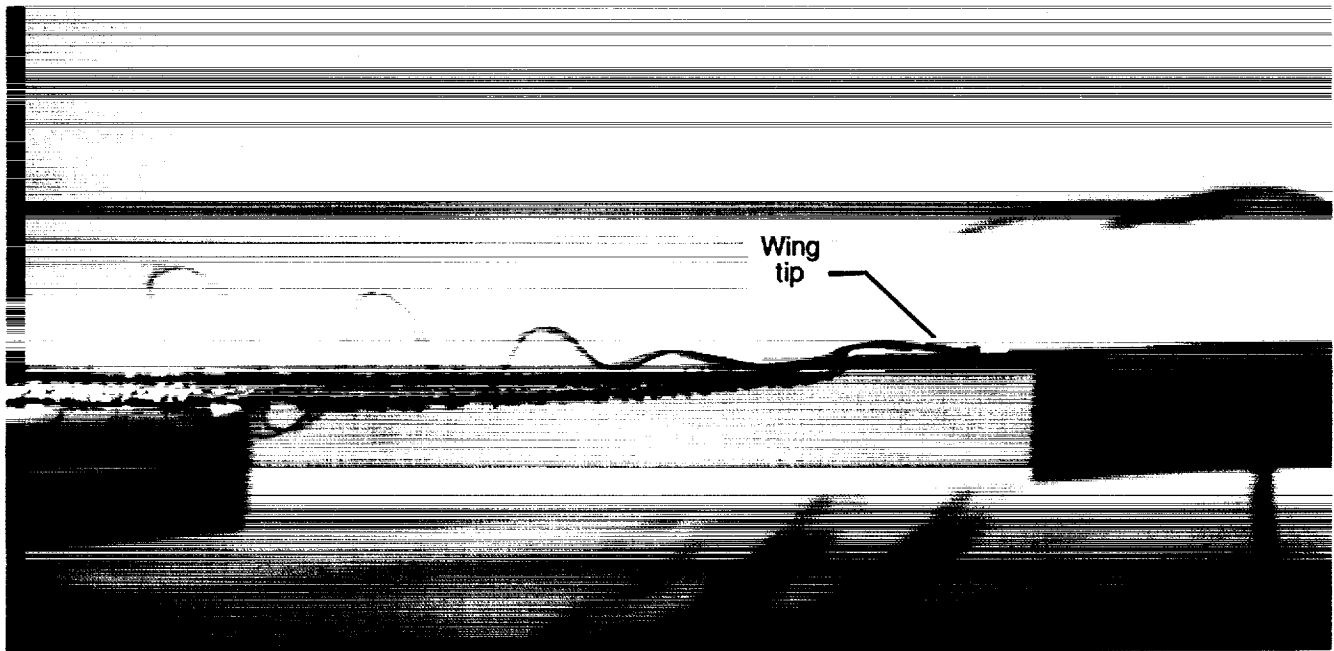
(a) $U_j/U_\infty = 2$ (aft jet only).
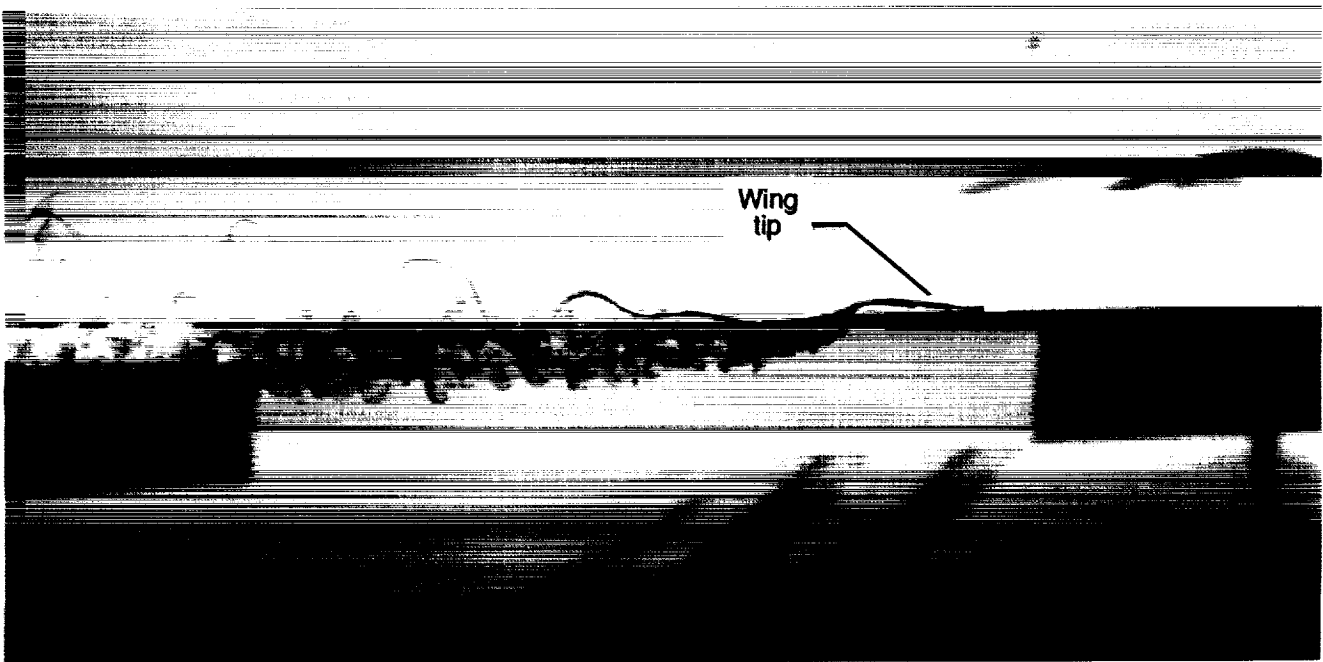
L-90-51

(b) $U_j/U_\infty = 4$ (aft jet only).

Figure 8. Side view of flow near tip D with $\alpha = 0°$.

16
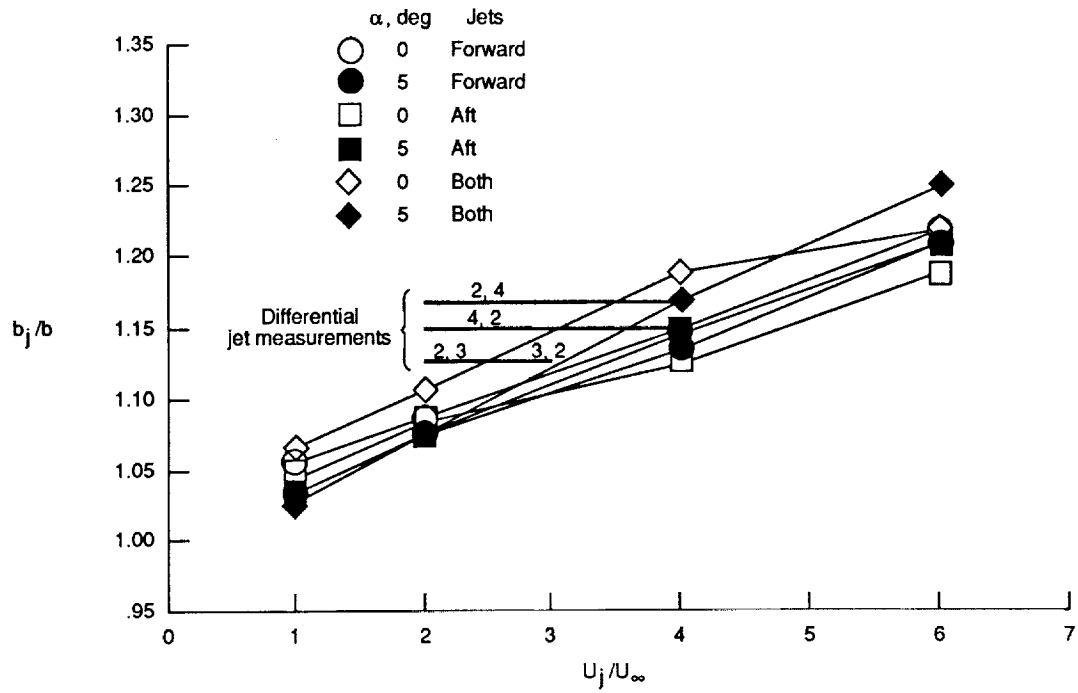
(a) Tip A.
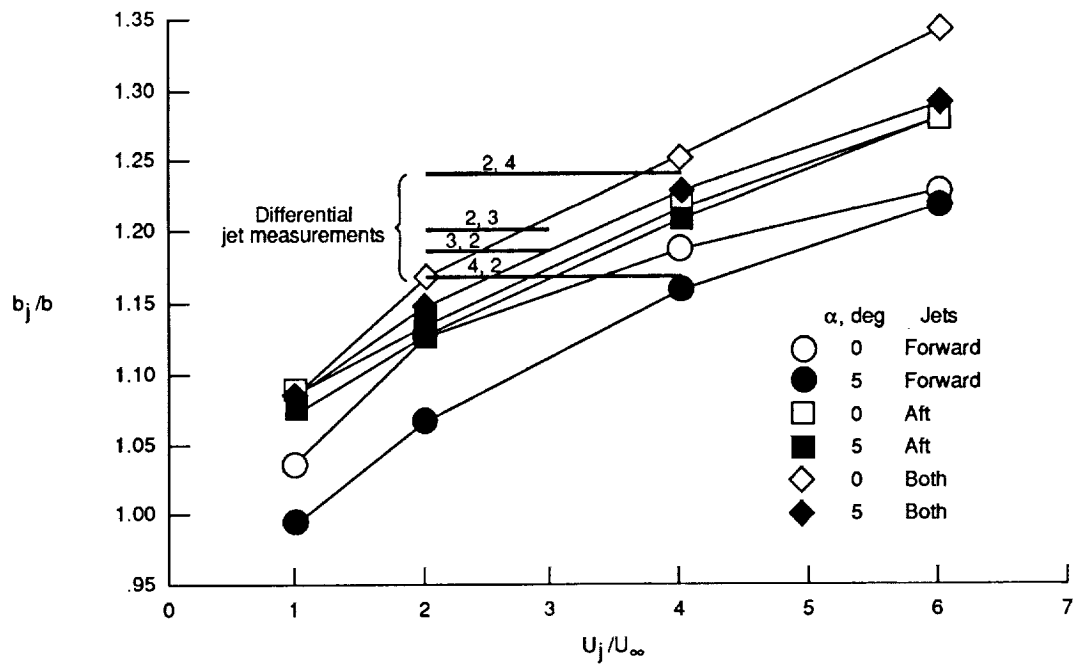
(b) Tip B.

Figure 9. Variation of jet span with velocity ratio.
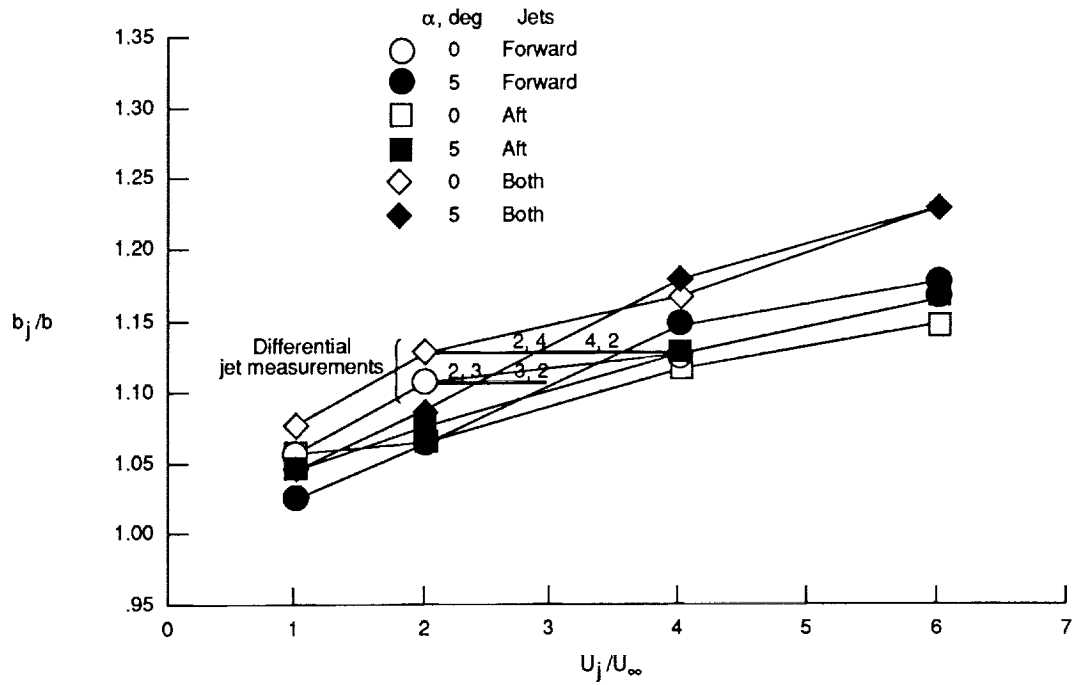
(c) Tip C.
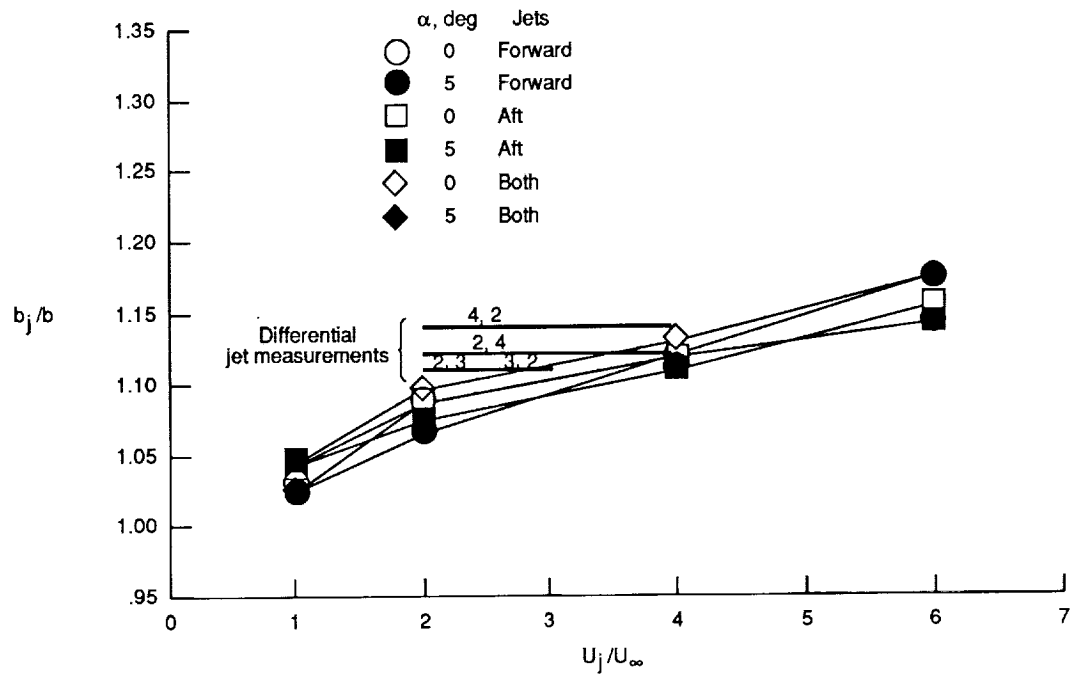
(d) Tip D.

Figure 9. Concluded.
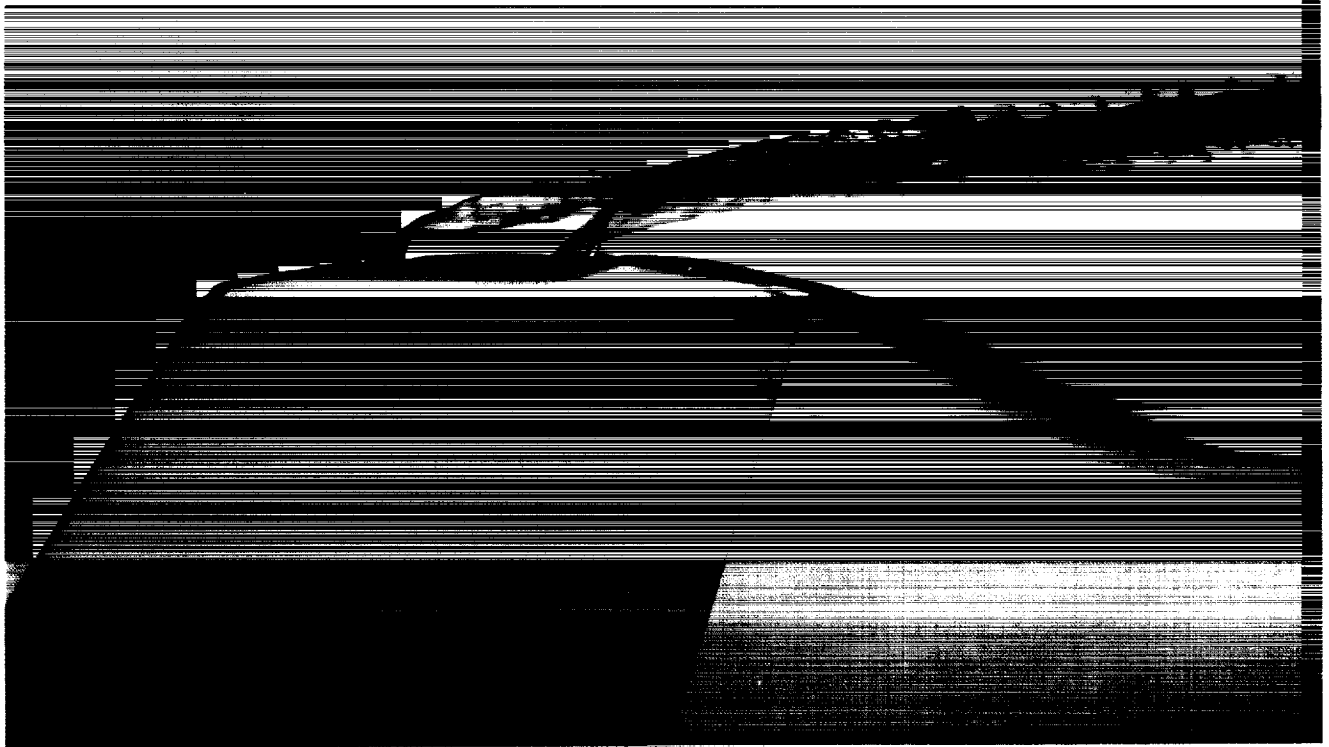
L-90-52

Figure 10. Plan view of flow near tip D with $\alpha = 0°$ and $U_j/U_\infty = 1$ (forward and aft jets).

L-90-53

Figure 11. Side view of flow near tip D with $\alpha = 5°$ and $U_j/U_\infty = 1$ (forward and aft jets).

19
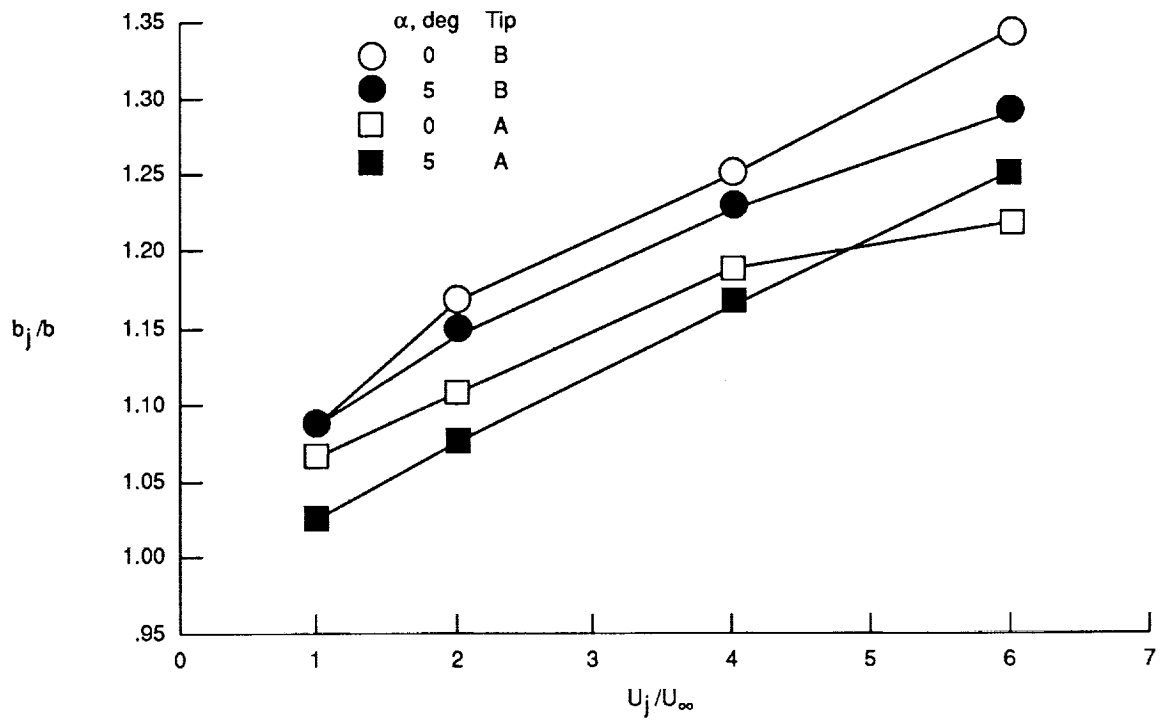
(a) Forward and aft jets.
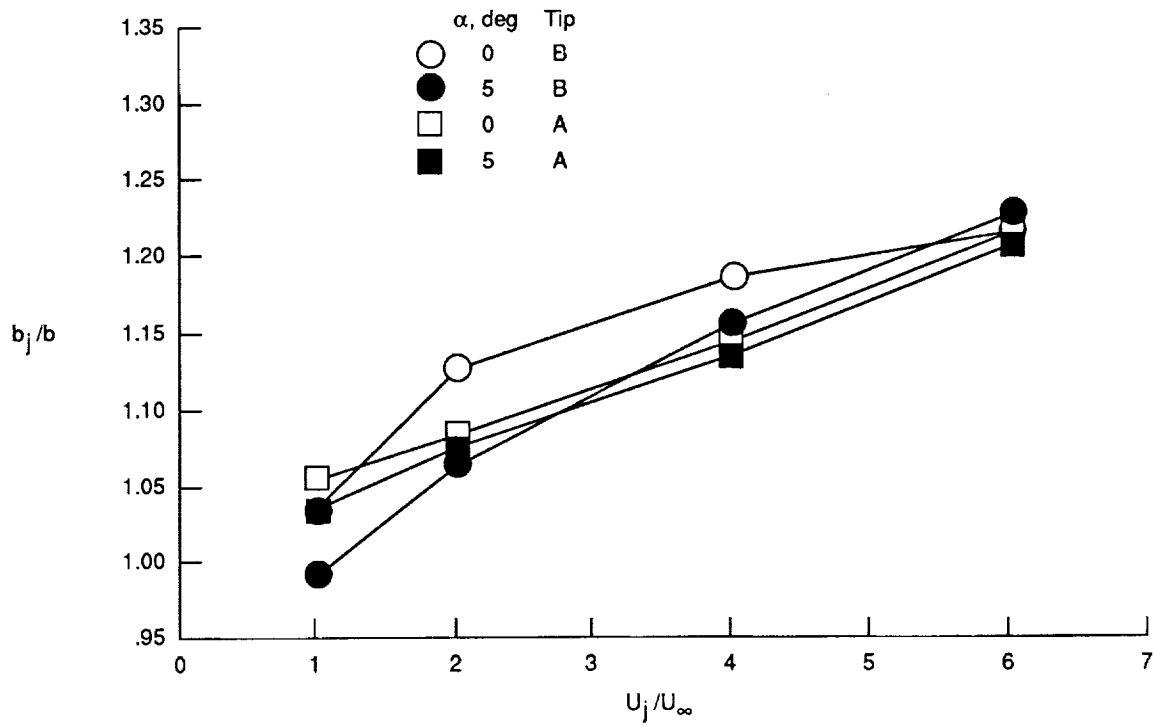
(b) Forward jets.

Figure 12. Effect of slot length on jet span.
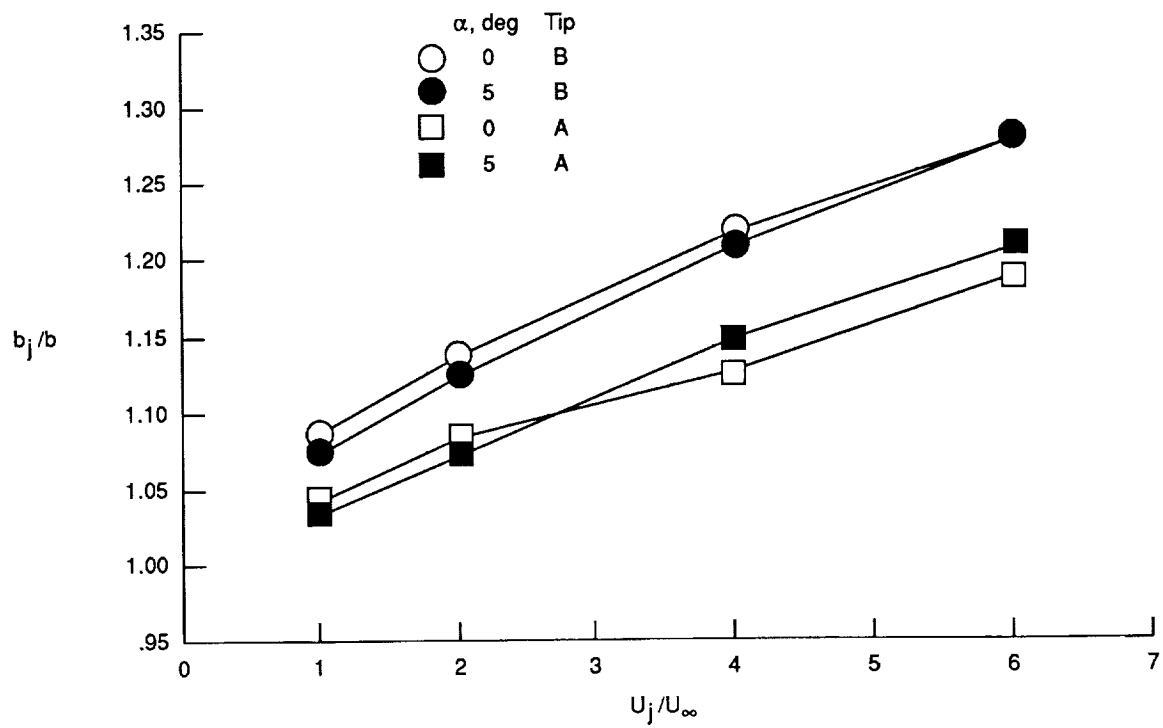
(c) Aft jets.

Figure 12. Concluded.
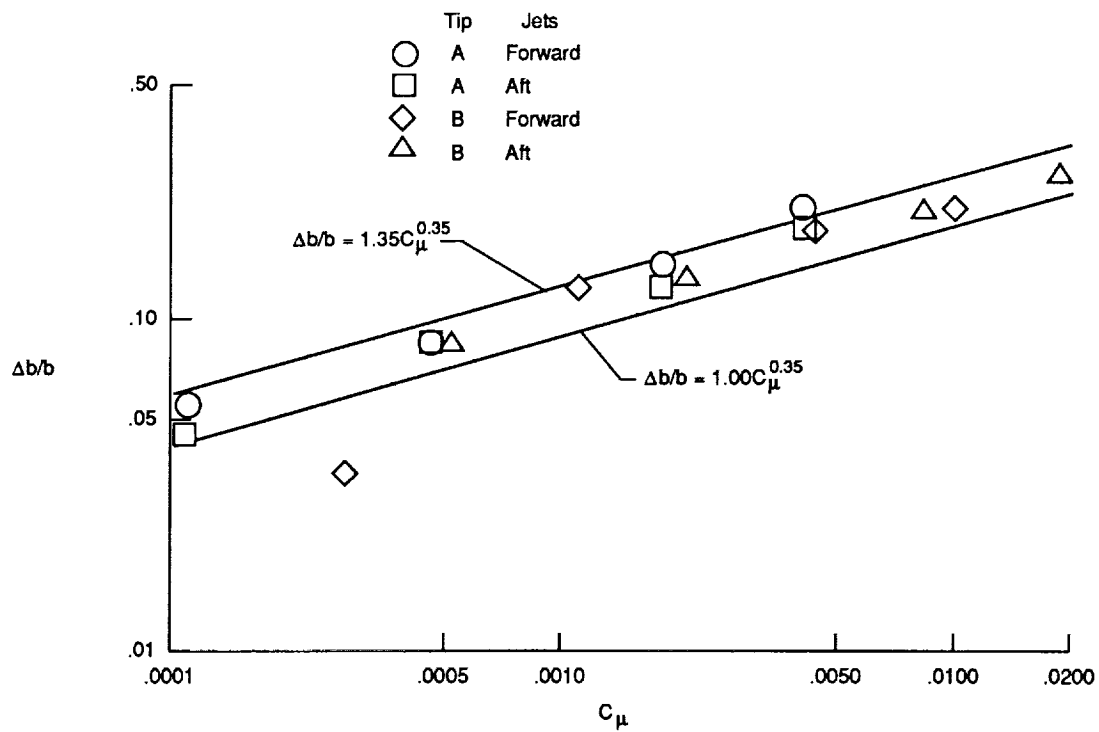
(a) $\alpha = 0°$.
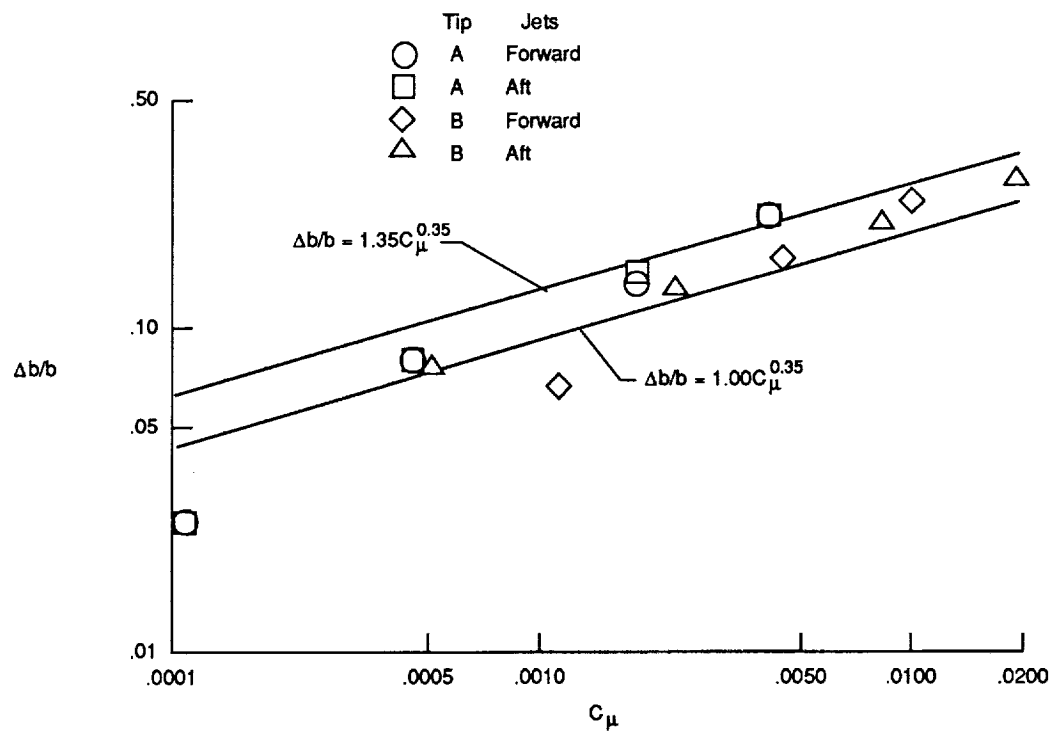
(b) $\alpha = 5°$.

Figure 13. Variation of jet span with jet momentum coefficient.
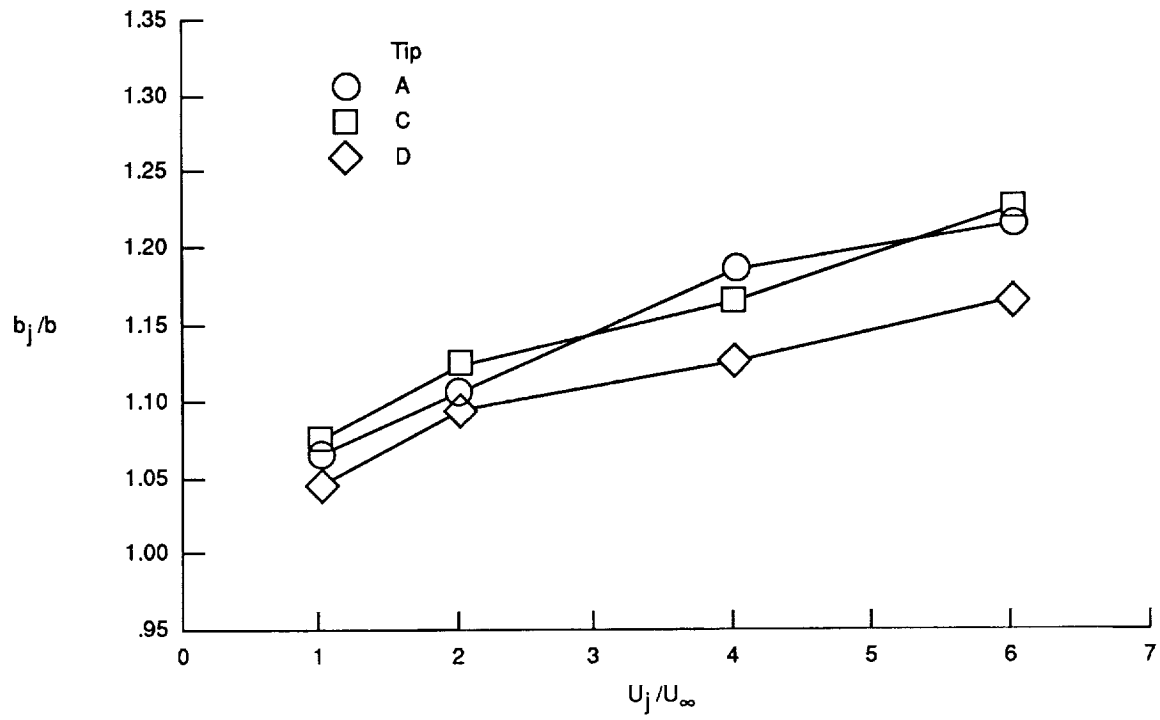
(a) $\alpha = 0°$, forward and aft jets.
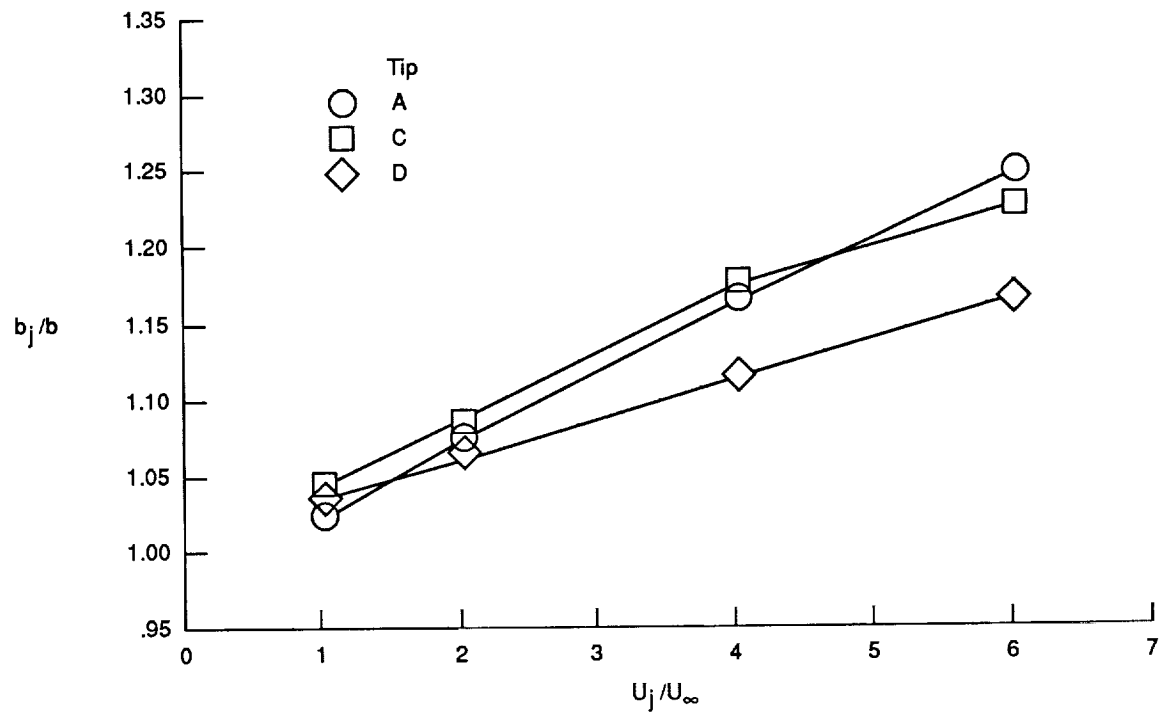
(b) $\alpha = 5°$, forward and aft jets.

Figure 14. Effect of blowing direction on jet span.
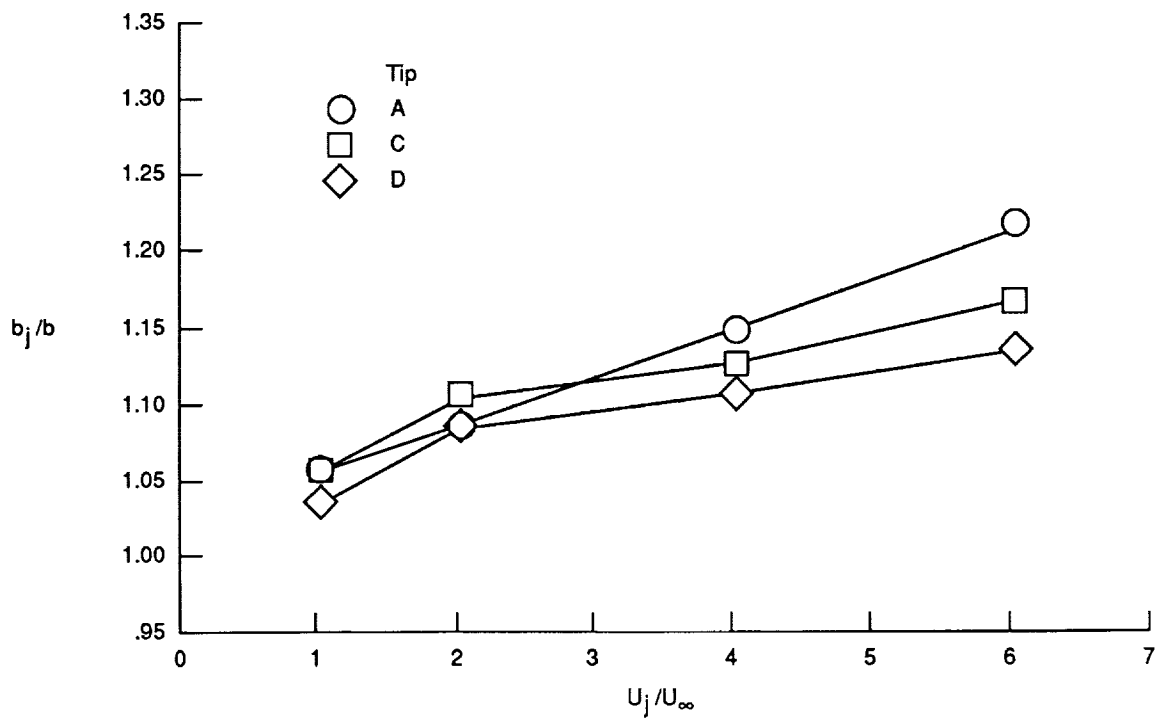
(c) $\alpha = 0°$, forward jet on.
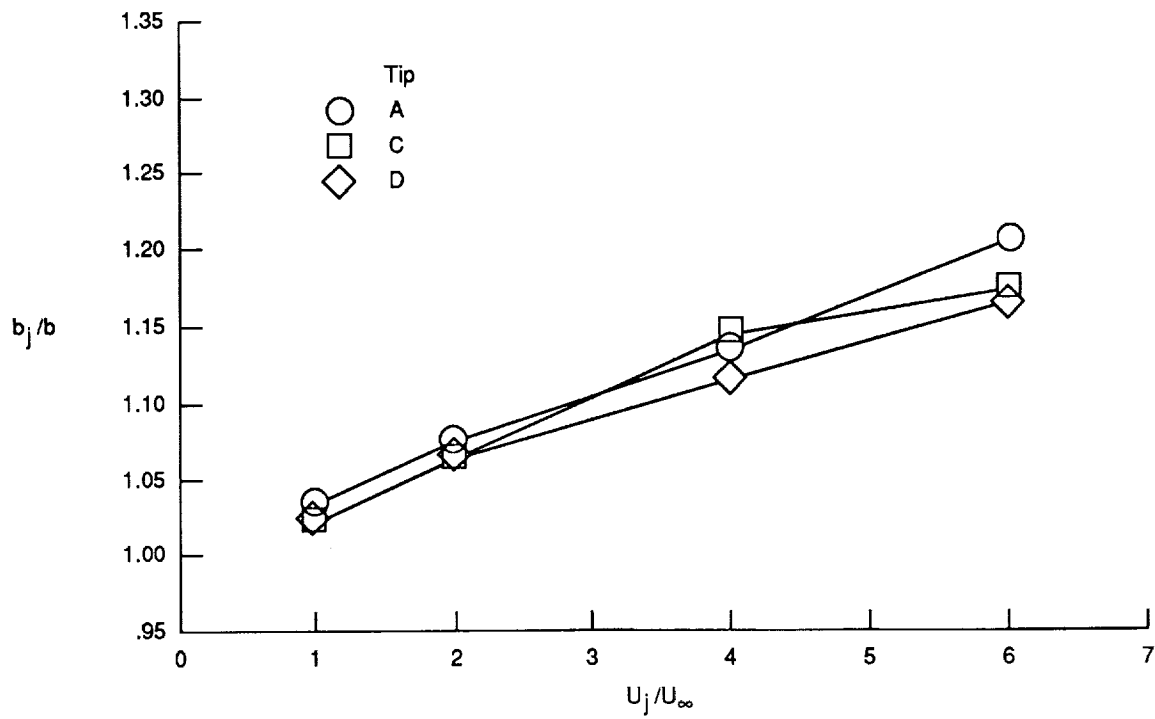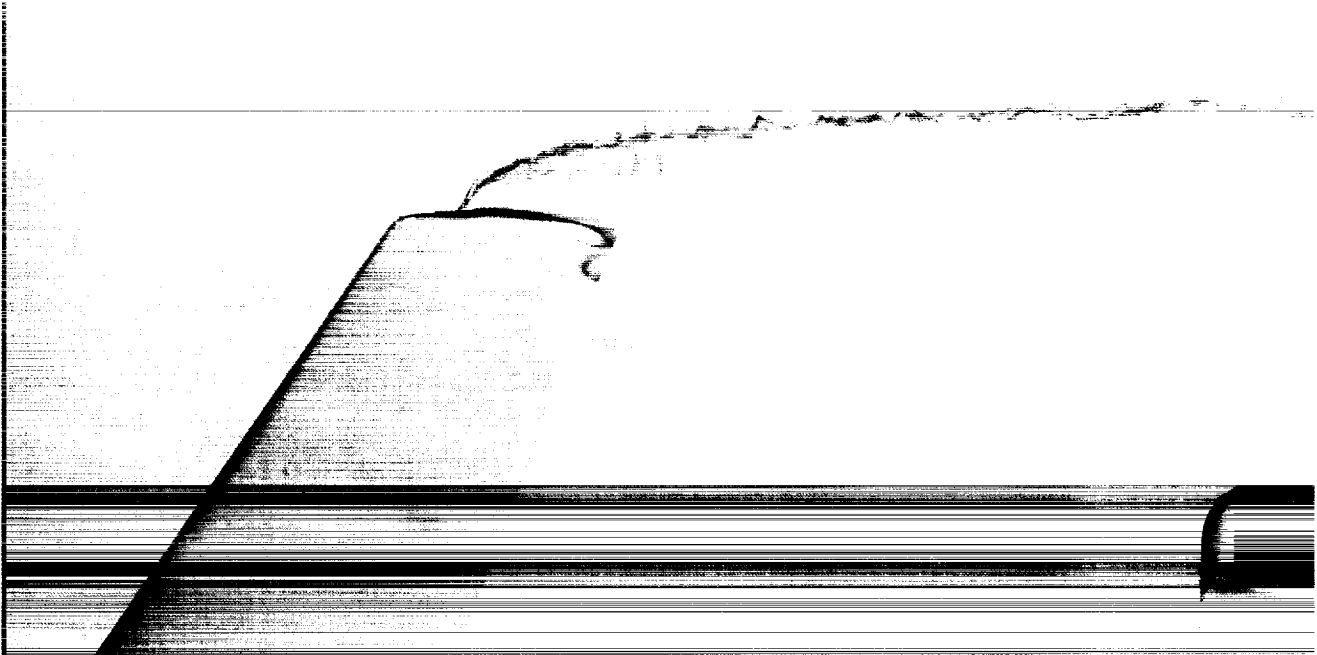

(d) $\alpha = 5°$, forward jet on.
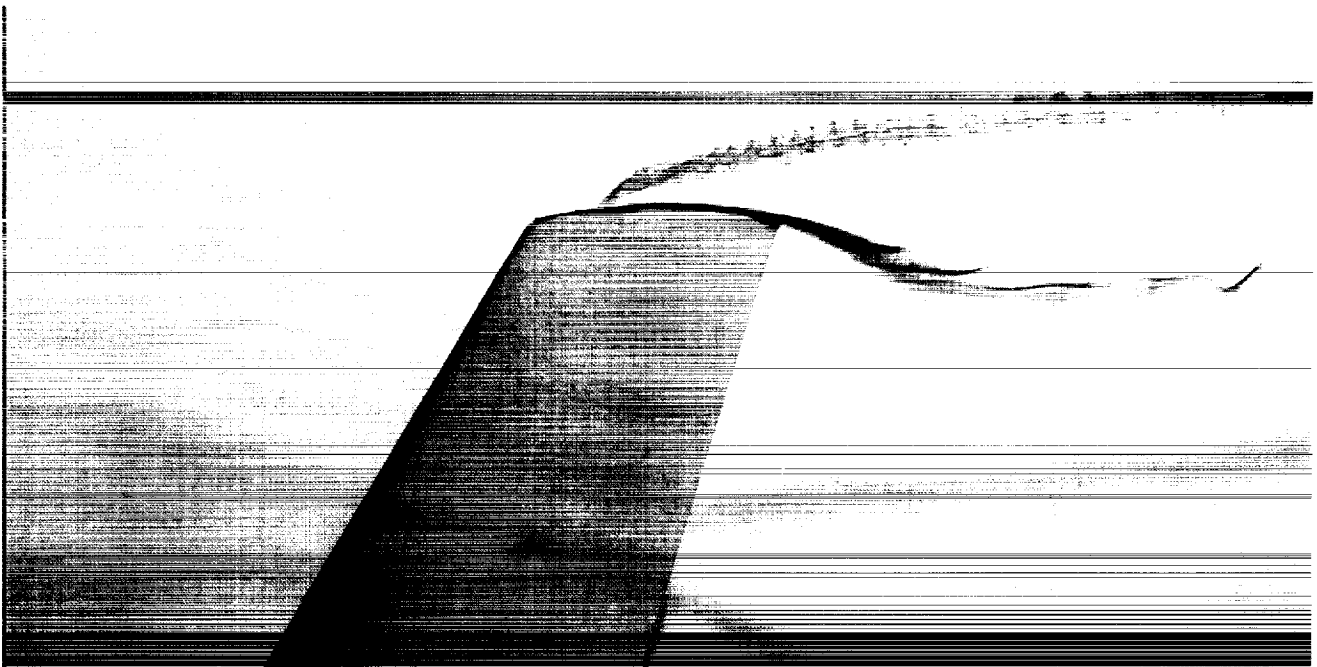
Figure 14. Continued.
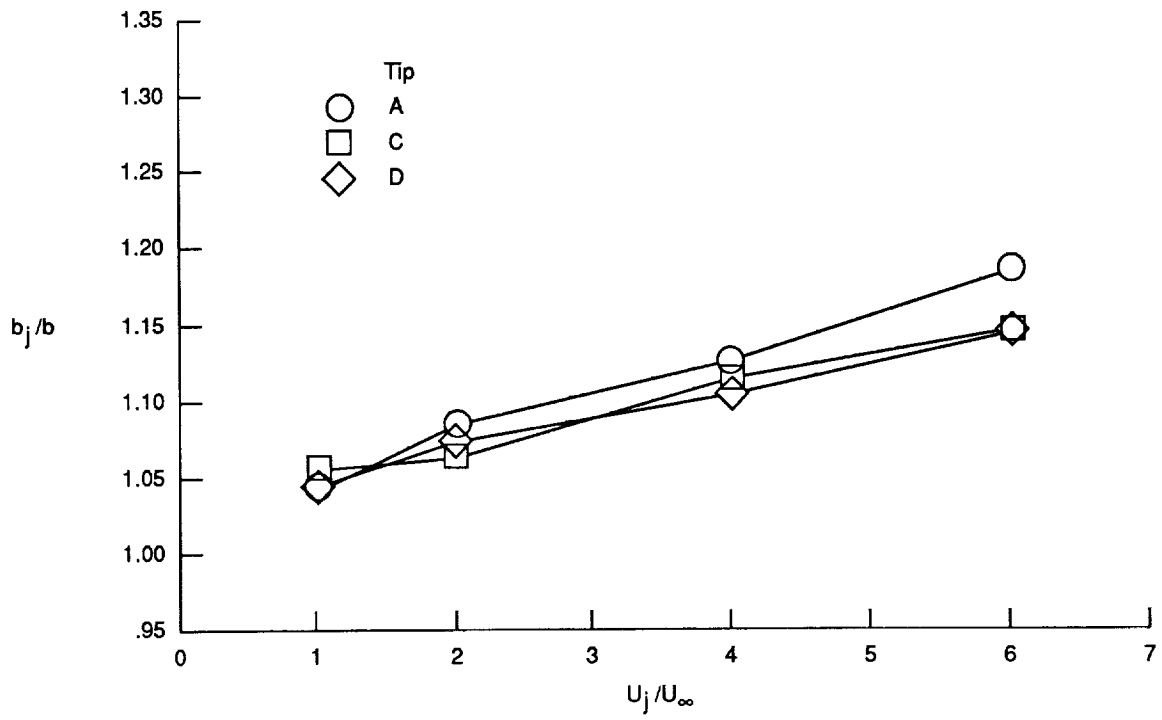
(e) $\alpha = 0°$, aft jet on.
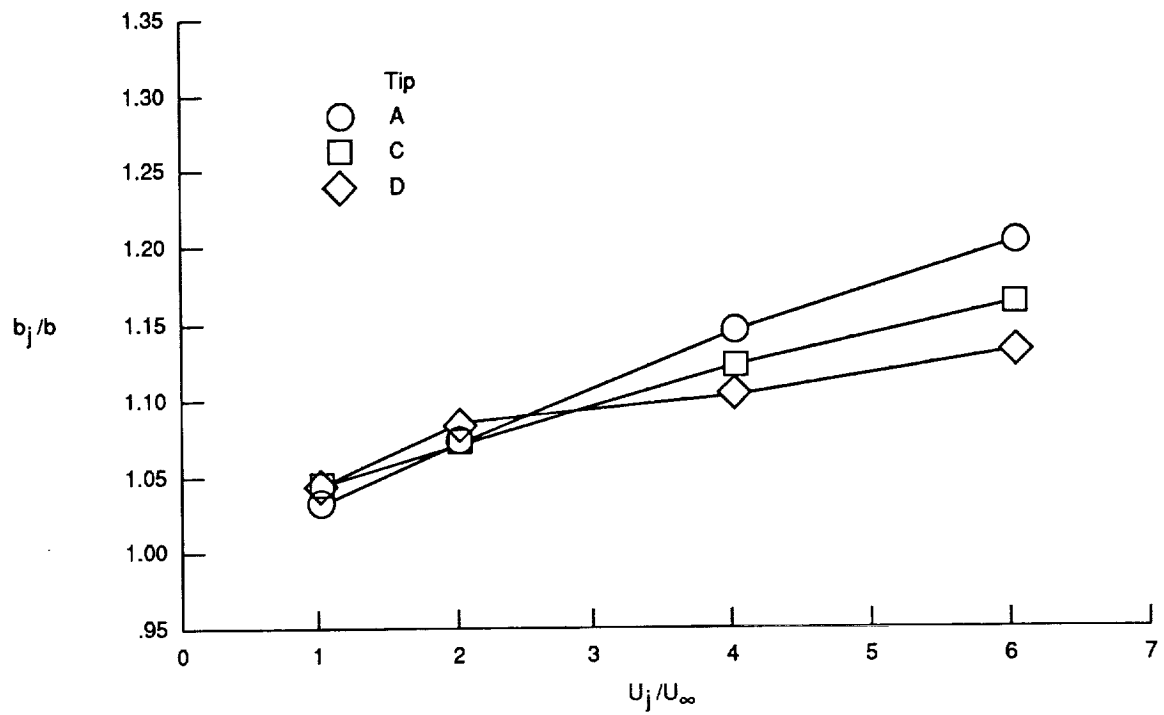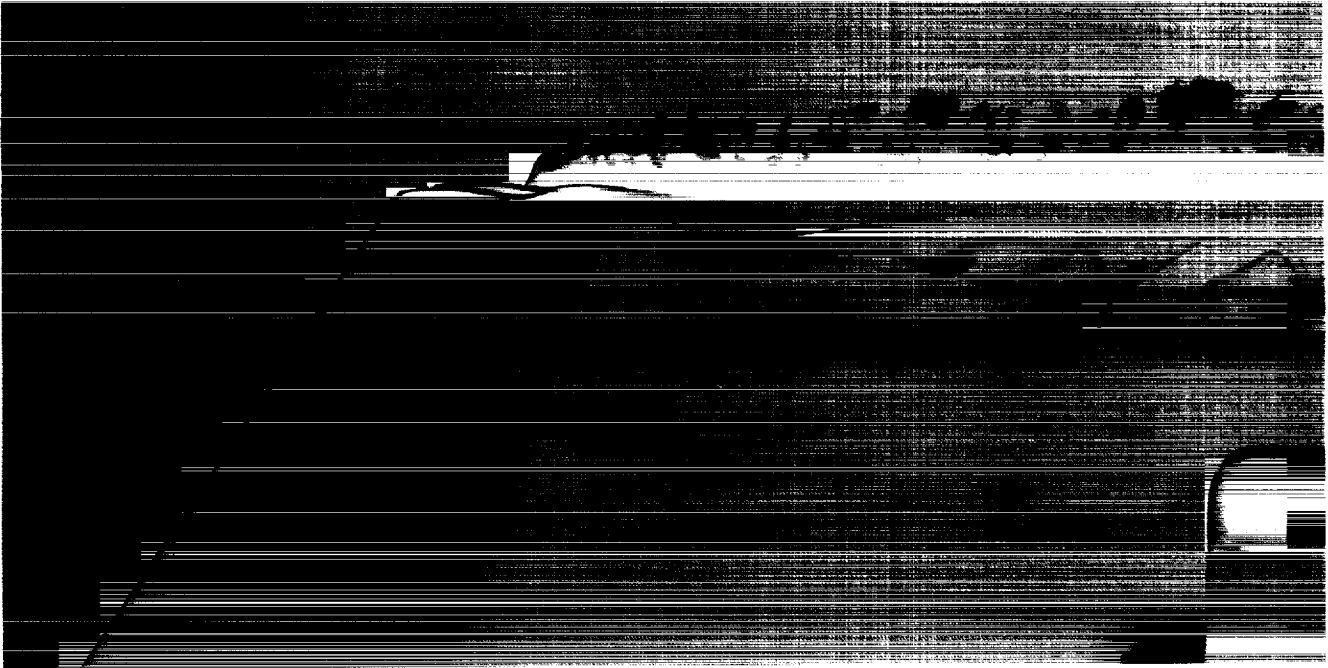

(f) $\alpha = 5°$, aft jet on.

Figure 14. Concluded.

(a) Tip C ($\psi_j = 0°$), forward jet on.

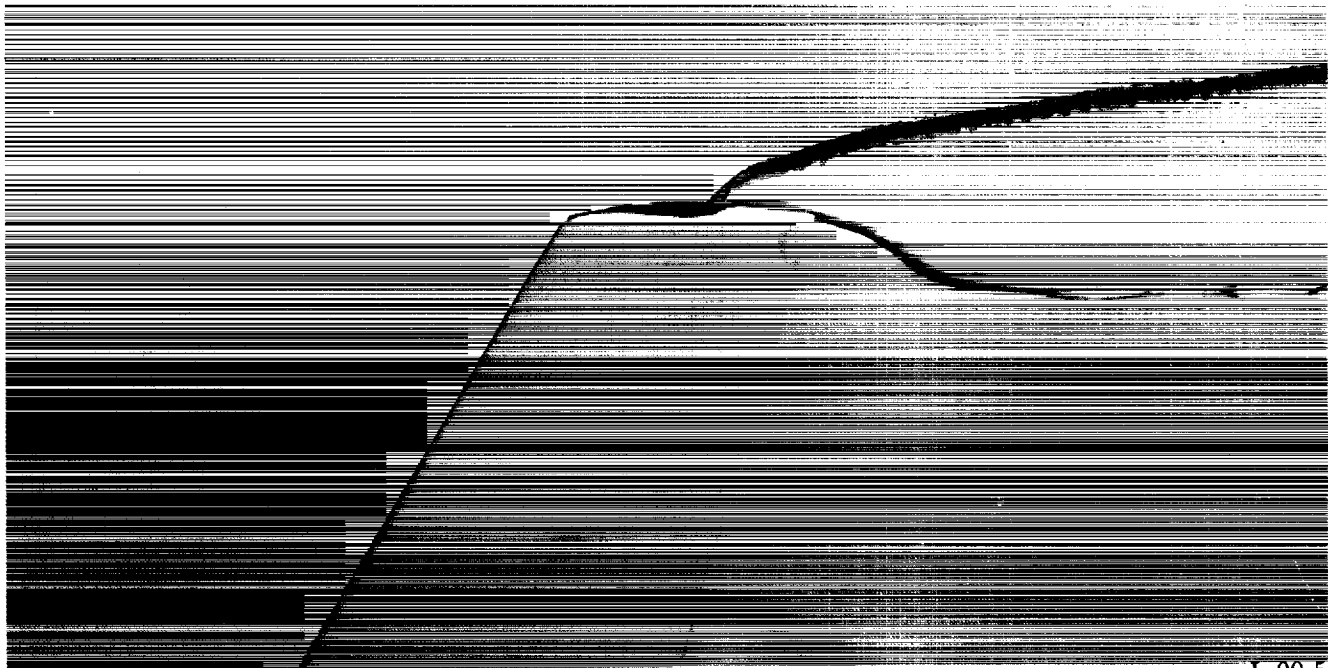
L-90-54

(b) Tip D ($\psi_j = 30°$), forward jet on.
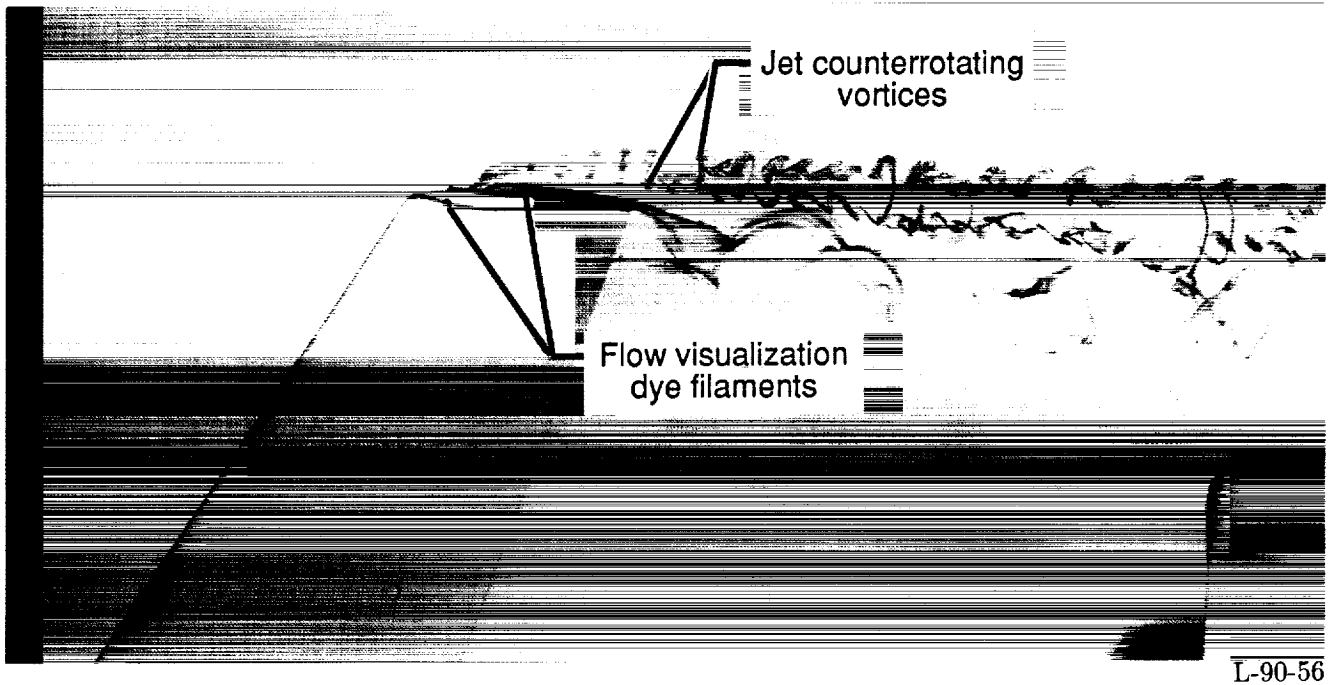
Figure 15. Effect of jet sweep on flow near tip.
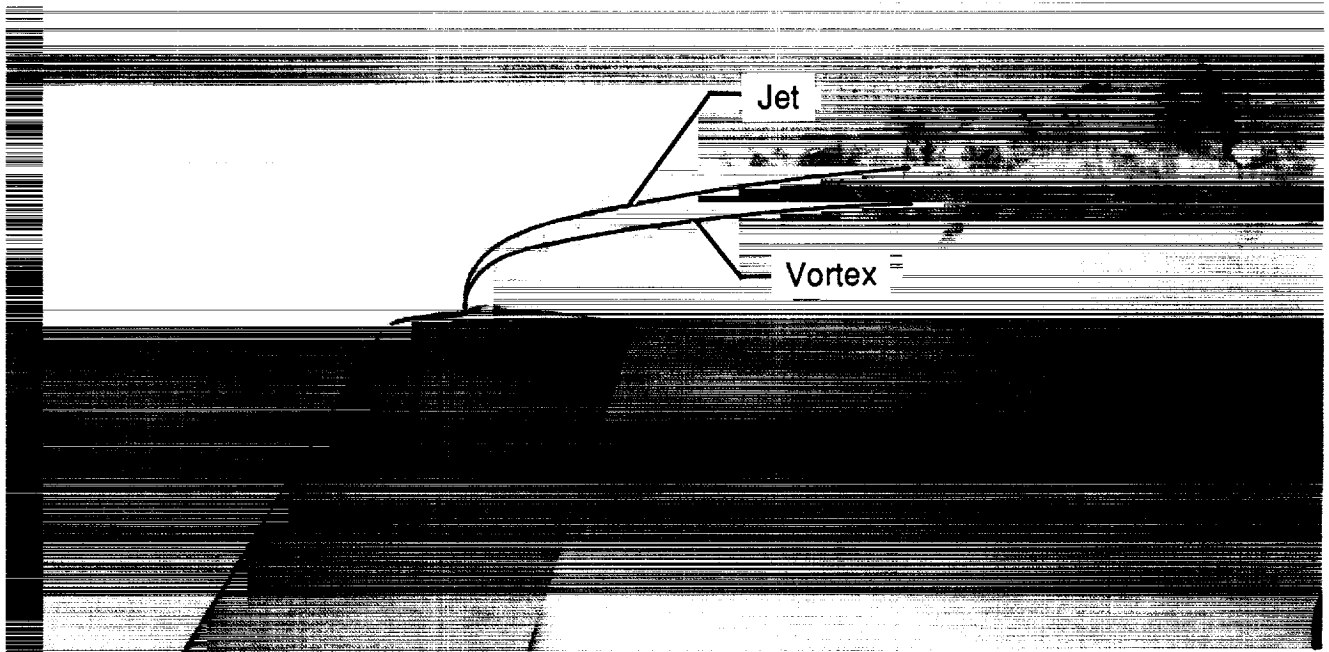
(c) Tip C ($\psi_j = 0°$), aft jet on.

L-90-55

(d) Tip D ($\psi_j = 30°$), aft jet on.

Figure 15. Concluded.

27

L-90-56

Figure 16. Counterrotating jet vortices. Tip C; $\alpha = 5°$; $U_j/U_\infty = 1$.

L-90-57

Figure 17. Comparison of flow field near tip A with empirical method of reference 6. $U_j/U_\infty = 4$; $\alpha = 0°$.

NASA
National Aeronautics and Space Administration

Report Documentation Page

1. Report No. NASA TM-4217	2. Government Accession No.	3. Recipient's Catalog No.

4. Title and Subtitle
Flow Visualization Studies of Blowing From the Tip of a Swept Wing

5. Report Date
November 1990

6. Performing Organization Code

7. Author(s)
Jeannette W. Smith, Raymond E. Mineck, and Dan H. Neuhart

8. Performing Organization Report No.
L-16767

9. Performing Organization Name and Address
NASA Langley Research Center
Hampton, VA 23665-5225

10. Work Unit No.
535-03-01-01

11. Contract or Grant No.

12. Sponsoring Agency Name and Address
National Aeronautics and Space Administration
Washington, DC 20546-0001

13. Type of Report and Period Covered
Technical Memorandum

14. Sponsoring Agency Code

16. Abstract
Flow visualization studies of blowing from the tip of a swept wing were conducted in the Langley 16- by 24-Inch Water Tunnel. Four wing tips, each with two independent blowing slots, were tested. The two slots were located one behind the other in the chordwise direction. The wing tips were designed to systematically vary the jet length, the jet in-plane exhaust direction (sweep), and the jet out-of-plane exhaust direction (anhedral). Each blowing slot was tested separately at two angles of attack and at four ratios of jet to free-stream velocity. Limited tests were conducted with blowing from both slots simultaneously. Blowing from the tip inhibited inboard spanwise flow on the upper wing surface near the tip. The jet path moved farther away from the tip as the ratio of jet velocity to free-stream velocity increased, and moved closer to the tip as angle of attack increased.

17. Key Words (Suggested by Authors(s))
Flow visualization
Wing-tip blowing
Water-tunnel tests

18. Distribution Statement
Unclassified—Unlimited

Subject Category 02

19. Security Classif. (of this report) Unclassified	20. Security Classif. (of this page) Unclassified	21. No. of Pages 29	22. Price A03